In vivo MR detection of vascular endothelial injury using a new class of MRI contrast agent

Tatsuhiro Yamamoto,[a] Kenjiro Ikuta,[a] Keiji Oi,[b] Kohtaro Abe,[b] Toyokazu Uwatoku,[b] Fuminori Hyodo,[c] Masaharu Murata,[a] Noboru Shigetani,[d] Kengo Yoshimitsu,[e] Hiroaki Shimokawa,[b] Hideo Utsumi[c] and Yoshiki Katayama[a,*]

[a]Department of Applied Chemistry, Faculty of Engineering, Kyushu University, Fukuoka 812-8581, Japan
[b]Department of Cardiovascular Medicine, Kyushu University Graduate School of Medical Sciences, Fukuoka 812-8582, Japan
[c]Laboratory of Bio-function Science, Graduate School of Pharmaceutical Sciences, Kyushu University, Fukuoka 812-8582, Japan
[d]Department of Radiology, Kyushu University Hospital, Fukuoka 812-8582, Japan
[e]Department of Clinical Radiology, Graduate School of Medical Sciences, Kyushu University, Fukuoka 812-8582, Japan

Abstract—A new class of dye-based MRI contrast agents, EB-DTPA-Gd, was designed and synthesized. The contrast agent was found to accumulate at the site of endothelial injury when the reagent was applied to isolated porcine blood vessels or in an ex vivo experiment using rat. In vivo MR detection of vascular endothelial injury was also successful in rat with its common carotid artery injured by balloon treatment. These results indicate that EB-DTPA-Gd is potentially useful for the diagnosis of vascular diseases.
© 2004 Elsevier Ltd. All rights reserved.

1. Introduction

Magnetic resonance imaging (MRI) has been used as an effective noninvasive diagnostic tool. For more effective diagnosis, various MRI contrast agents have been reported.[1,2] In T1-weighted MR imaging, gadolinium ion-chelate complexes have primarily been applied, as the gadolinium ion interacts with hydrogen in water molecules and enhances the T1-relaxation.[2] As a result, clearer images can be obtained when using these gadolinium ion complexes. In this context, many kinds of site-specific MR-contrast agents have been developed.[3-6] These agents have been designed with the intent of conjugating the targeting unit with the MR detection unit. In the site-specific MRI strategy, blood vessel is one of the most promising targets, as diagnosis of vascular disease in its early stages is essential to a successful treatment intervention. However, the development of such vascular disease-specific MRI has not yet been

achieved. Various biomolecules such as antibodies for integrin,[3,4] ICAM-1,[5] or fibrin[6] that interact with proteins related to vascular disease have been used in the design of such MRI reagents. The use of these biomolecules, however, has proved to be impractical in terms of cost and volume of the agents. Another possible approach involves the use of synthesized organic molecules. It has been found that MS-325 (4,4-diphenylcyclohexyl phosphodiester Gd-DTPA derivative) forms a high-molecular weight complex with albumin before its adsorption onto plaque. As such, this molecule has been applied to the imaging of blood vessels in the SLE mouse.[7]

We, however, have focused our attention on endothelium lesions as a target of the MRI contrast agent for the diagnosis of vascular disease. The vascular endothelium plays an important role in the regulation of vascular homeostasis. As such, any damage to the endothelium often leads to a serious vascular disorder such as spasms in myocardial infarction.[8] In these lesional sites, it may be possible that a certain type of molecule could interact with the extracellular matrix or the smooth muscle layer through hydrophobic or electrostatic interactions due to a loss or weakening of endothelial regulation of substances.[9] We therefore
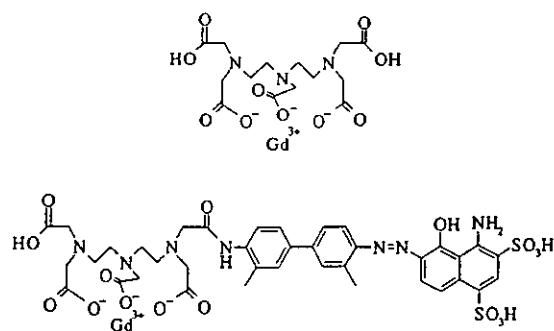
Figure 1. Chemical structure of MRI contrast agents, Gd-DTPA and EB-DTPA-Gd.

screened various organic dyes that have been used in histochemistry and found some azo-dyes that were selectively adsorbed to endothelium-denuded regions in an isolated porcine aorta sample. These dyes can interact with proteins or various tissues probably due to their good hydrophilicity or hydrophobicity balance, although accurate molecular mechanism of the binding has not been elucidated. Of these dyes, we have found Evans Blue capable of most effectively identifying the endothelium-injured region.

We have recently reported the synthesis and basic properties of an endothelium lesion-specific MRI contrast agent, EB-DTPA-Gd (Fig. 1).[10] The reagent was designed using the chemical structure of Evans Blue. This agent selectively accumulates on the endothelium-denuded surface of the porcine aorta section and enhances its signal intensity of the surface, as observed on the T1-weighted MR images.

In the present study, we applied the vascular endothelial lesion-specific contrast agent, EB-DTPA-Gd, to living rat for both ex vivo and in vivo MR imaging. First, the isolated porcine blood vessels, the endothelium of which is partially removed by scalpels, was treated with EB-DTPA-Gd in the presence of serum proteins. We next attempted ex vivo and in vivo MR imaging of the rat vascular injury at the common carotid artery, which was injured with a balloon catheter.

2. Experimental

2.1. In vitro evaluation of an isolated porcine aorta treated with EB-DTPA-Gd in the presence and absence of serum protein

A vascular endothelial lesion-specific MRI contrast agent module, EB-DTPA, was successfully synthesized, as described previously.[10,11] Complexation of EB-DTPA with gadolinium ion was achieved as follows; EB-DTPA was dissolved at 10 mM in water containing a ca. 1.5 M excess of Na_2CO_3 and equimolar gadolinium chloride was added. After adjustment to pH 7, the solution was lyophilized to obtain the desired MRI contrast agent

solid, EB-DTPA-Gd. To evaluate the effects of serum proteins, EB-DTPA-Gd was dissolved in porcine serum[12] or pure water to a final concentration of 10 mM.

The specimens of porcine aorta were extracted and opened to a rectangular shape. The endothelium of the left half of the aorta was then carefully removed by scalpel (Fig. 2a). The blood vessel section was stained with each MRI contrast agent solution for 10 s and washed with saline. The aorta section was then evaluated by MR imaging (1.5 T MAGNETOM VISION system (SIEMENS, Germany), T1-weighted spin-echo, TR/TE = 400/14 m s, 3 mm slice thickness, field-of-view 50 mm, and dot matrix 128*256). The obtained MRI image was analyzed using NIH Image software.

2.2. Ex vivo or in vivo evaluation of EB-DTPA-Gd using the rat

A solid EB-DTPA-Gd was dissolved in saline to a final concentration of 24 mM. Rats (about 300 g) were anesthetized with intraperitoneal sodium pentobarbital (50 mg/kg), and then a balloon injury of the left carotid artery was made as previously described.[13] The MRI contrast agent solution was injected to the rat via the jugular vein at 160 µmol/kg. In the ex vivo experiment, the right and left common carotid arteries were extracted after 10, 30, or 120 min of reagent injection. The arteries were then opened and fixed on glass plate, and evaluated T1-weighted MR images using the same parameters as those for the in vitro experiment as described earlier.
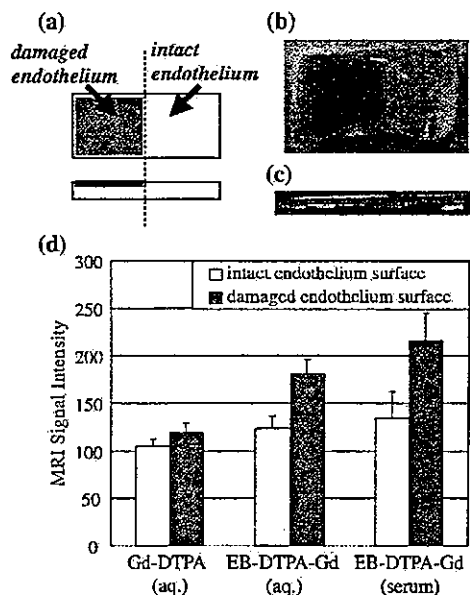

Figure 2. (a) Schematic illustration of the porcine aorta section. The left-half endothelium was removed, and the right half was intact. (b and c) The photograph and T1-weighted MR image (side view) of porcine aorta section stained with EB-DTPA-Gd in the presence of serum proteins. (d) Comparison of the surface MRI signal intensities of the porcine aorta section. The error bars represent the standard deviation ($N = 3$).
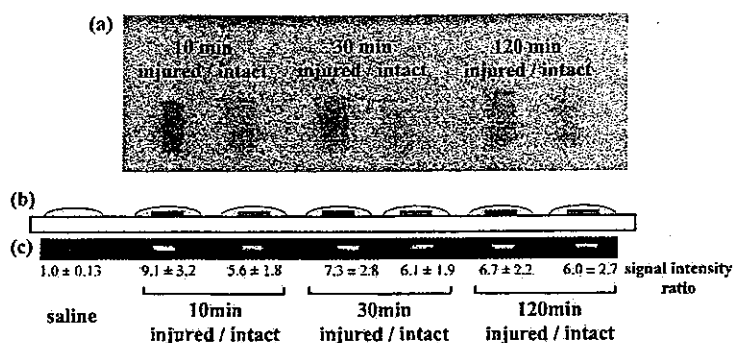
221

Figure 3. Ex vivo results for the opened common carotid arteries of the rat after the EB-DTPA-Gd injection via jugular vein. (a) Photograph of the extracted rat common carotid arteries at the elapsed times (10–120 min) after the injection of EB-DTPA-Gd. (b and c) Schematic illustration and MR image of both arteries dipped into saline (7 μL). The signal intensity ratio was calculated by comparing the MRI signal intensities of each artery in the saline drop with that of the saline drop alone.

The similar procedures were repeated for in vivo MR imaging of another rat. The animal was anesthetized and kept alive after its left carotid artery being injured by balloon catheter method as described.[13] After the injection of the MRI contrast agents, serial T1-weighted spin-echo MR images of the left carotid artery through transaxial plane were obtained. MR equipment used for this in vivo experiment was a 0.2 T unit (MRP-20, Hitachi, Japan). The parameters for the sequence were as follows; TR/TE = 500/25 m s, 2.5 mm slice thickness, field-of-view 200 mm, and dot matrix 256*192. As a control, 24 mM Gd-DTPA saline solution was used in a similar manner.
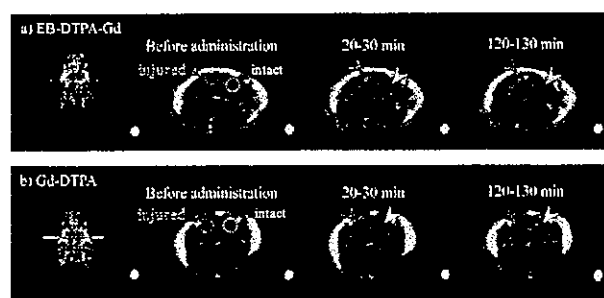

Figure 4. In vivo MR images of the rat with administration of (a) EB-DTPA-Gd and (b) Gd-DTPA via left femoral vein. The left common carotid artery was injured, and the right one was intact. The arrows in the figure indicate each artery.

3. Results and discussion

Various dyes, including Evans Blue and Congo Red, have been reported to bind to serum proteins.[14] It therefore seemed likely that EB-DTPA-Gd would also bind to serum proteins. We therefore investigated whether the presence of the serum proteins affect the characteristics of EB-DTPA-Gd, namely ability to accumulate at the sites of endothelial injury. The endothelium condition is schematically illustrated in Figure 2a. In the presence of serum proteins, EB-DTPA-Gd selectively accumulated on the endothelium injured surface (Fig. 2b). T1-weighted MR images revealed significant signal enhancement only on the endothelium-removed surface of the specimens, treated both with porcine serum and pure water solution of EB-DTPA-Gd (Fig. 2c and d). This result indicates that the serum does not affect the endothelium lesion-specific binding of EB-DTPA-Gd. The nonspecific binding of EB-DTPA-Gd slightly increased if compared with the result in the absence of serum proteins. This increase may be due to formation of the high-molecular weight complex of EB-DTPA-Gd with serum proteins.

For the next experiment, ex vivo MR imaging of the vascular endothelium injury was performed. In ex vivo study, carotid arteries with and without endothelial injury were clearly distinguished by the presence and absence of EB-DTPA-Gd accumulation, respectively, both

by macroscopic observation and by T1-weighted MR images as well (Fig. 3). Figure 3c shows the MR image of the same section of aorta. The MRI signal intensity of the extracted left common carotid artery was largest after 10 min of the EB-DTPA-Gd injection. As time elapsed, the signal intensity of the left carotid artery gradually decreased, and 120 min after injection of EB-DTPA-Gd, it was almost the same as that of the right (intact side) carotid artery. The signal intensity of the right carotid artery slightly increased after EB-DTPA-Gd injection as compared to the baseline level, probably due to nonspecific binding of the contrast agent to the intact endothelium. As a site-specific contrast agent based on small organic molecule, MS-325 has been reported. The agent recognizes a inflammation site in blood vessels of SLE mice.[7] However the mechanism of the specific accumulation at the target site totally depends on the property of albumin, because the agent is carried by albumin. On the other hand, our compound possesses the recognition ability of the endothelial injury by itself.[10] Although the accurate mechanism of the recognition has not been clear.

For the final experiment, in vivo MR detection of the rat vascular injury was performed. The in vivo MRI results are shown in Figure 4. With the injection of EB-DTPA-Gd, the injured left common artery was clearly enhanced compared with the right intact common artery.

Gd-DTPA, however, did not enhance the MRI signal in either injured or intact artery. In contrast to the results of ex vivo study, the largest signal intensity of the endothelial injury was observed 120 min after EB-DTPA-Gd injection. We expected that the difference may be caused by the infiltration of the contrast agent into the tissue through the injured blood vessel surface.

4. Conclusion

Endothelial lesions are essential to the early-stage development of vascular diseases. We designed and synthesized a new dye-based MRI contrast agent, EB-DTPA-Gd, for the detection of such endothelium lesional sites. EB-DTPA-Gd was found to selectively bind to the target regions in extracted porcine aorta or living rat common carotid artery, even in the presence of serum or the blood stream. Finally, we preliminarily succeeded in carrying out noninvasive detection of injured blood vessel regions in living rat using an in vivo MRI technique. The contrast agent and the concept for the design using organic dye will be potentially useful in the development of a reliable diagnostic system that can detect vascular disease in its early stages.

Acknowledgements

References and notes

1. Caravan, P.; Ellison, J. J.; McMurry, T. J.; Lauffer, R. B. Chem. Rev. 1999, 99, 2293.
2. Piguet, C.; Bunzli, J. C. G. Chem. Soc. Rev. 1999, 28, 347.
3. Sipkins, D. A.; Cheresh, D. A.; Kazemi, M. R.; Nevin, L. M.; Bednarski, M. D.; Li, K. C. Nat. Med. 1998, 4, 623.
4. Anderson, S. A.; Rader, R. K.; Westlin, W. F.; Null, C.; Jackson, D.; Lanza, G. M.; Wickline, S. A.; Kotyk, J. J. Magn. Reson. Med. 2000, 44, 433.
5. Sipkins, D. A.; Gijbels, K.; Tropper, F. D.; Bednarski, M.; Li, K. C.; Steinman, L. J. Neuroimmunol. 2000, 104, 1.
6. Yu, X.; Song, S. K.; Chen, J.; Scott, M. J.; Fuhrhop, R. J.; Hall, C. S.; Gaffney, P. J.; Wickline, S. A.; Lanza, G. M. Magn. Reson. Med. 2000, 44, 867.
7. Herborn, C. U.; Waldschuetz, R.; Lauenstein, T. C.; Goyen, M.; Lauffer, R. B.; Moeroey, T.; Debatin, J. F.; Ruehm, S. G. Invest. Radiol. 2002, 37, 464.
8. Ross, R. N. Engl. J. Med. 1999, 340, 115.
9. Bazzoni, G.; Martinez, E. O.; Dejana, E. Trends Cardiovasc. Med. 1999, 9, 147.
10. Yamamoto, T.; Ikuta, K.; Oi, K.; Abe, K.; Uwatoku, T.; Murata, M.; Shigetani, N.; Yoshimitsu, K.; Shimokawa, H.; Katayama, Y. Anal. Sci. 2004, 20, 5.
11. Precursor of the EB-DTPA, DMB-DTPA, was synthesized by the coupling of mono-Boc protected dimethylbenzidine and DTPA anhydride and was obtained as a TFA salt. The synthesis of EB-DTPA was performed as described below. All reactions were performed in an ice bath. DMB-DTPA·4TFA (0.53 g, 0.51 mmol) was dissolved in water (15 mL) containing HCl (1.52 mmol). Sodium nitrite (35 mg, 0.51 mmol) was then added in small portions, followed by stirring for 20 min. The diazonium salt solution was added dropwise into 15 mL of an aqueous 1-amino-8-naphthol-2,4-disulfonic acid (0.17 g, 0.51 mmol) solution containing sodium bicarbonate (0.43 g, 4.08 mmol), and then stirred for 3 h. The reaction mixture was lyophilized. The obtained solid was redissolved in water (10 mL), and the desired product was precipitated by concd hydrochloric acid. The precipitate was collected and dried under reduced pressure (0.36 g, 78%). The chemical structure was determined by ^{1}H NMR and elemental analysis.
12. Porcine serum was prepared as follows. Extracted porcine blood was centrifuged at 3000 rpm for 10 min to remove hemocyte. The concentrations of serum proteins obtained as the supernatant were determined to be 55 mg/mL (albumin: 33 mg/mL) by entrusting them to an outsourcer.
13. Uwatoku, T.; Shimokawa, H.; Abe, K.; Matsumoto, Y.; Hattori, T.; Oi, K.; Matsuda, T.; Kataoka, K.; Takeshita, A. Circ. Res. 2003, 92, e62.
14. Tsopelas, C.; Sutton, R. J. Nucl. Med. 2002, 43, 1377.

Bio Medical Quick Review Net

No. 4009

血管内皮障害部位を特異的に診断できる造影剤

片山　佳樹[1]・山本　竜広[2]・下川　宏明[3]

九州大学工学研究院応用化学部門　教授[1]

九州大学大学院工学研究科[2]

九州大学医学研究院循環器内科　助教授[3]

血管内皮障害部位を特異的に診断できる造影剤

片山　佳樹[1]・山本　竜広[2]・下川　宏明[3]

九州大学工学研究院応用化学部門　教授[1]

九州大学大学院工学研究科[2]

九州大学医学研究院循環器内科　助教授[3]

　動脈硬化やバルーン療法後に引き起こされる血管炎症部位は，循環器系疾患の原因部位である。これまで，このような部位を特異的に診断できる有効な手法は存在しなかった。われわれは，このような病変部位が炎症性に内皮が傷害されていることに着目し，色素分子を利用することで，安価でかつ高性能に当該部位に吸着し，MRI法により画像診断できる新しい造影剤を開発した。本造影剤は，摘出血管およびラット体内において内皮障害モデル部位に特異的に吸着し，検出することが可能であった。

key words

核磁気共鳴イメージング，MRI，血管造影剤，有機色素，
動脈硬化，循環器系疾患，ガドリニウム錯体，臨床診断，プラーク

はじめに

　社会の高齢化が進み，動脈硬化を起因とする循環器系疾患は，今後ますます重要な診断・治療対象になると考えられる。血管の攣縮は血管のある部分が過収縮を起こして血流を妨げる現象であるが，血管のどの部分でも起こりうるというものではなく，動脈硬化が促進することにより血管壁に進入したマクロファージなどが原因で起こる炎症部分で特異的に発症する。従って，このような炎症部位をあらかじめ診断できれば，発作を起こす前に治療が可能となる。しかしながら，現在そのような実用的診断法はなく，発作後に血管を造影して攣縮箇所を診断するしかないのが現状である。また，血管が閉塞した箇所は，カテーテルを挿入してバルーン処置などにより血管を拡張させるが，その際，血管内面を傷害してしまい，これが炎症や内皮肥厚の原因となる。そこで，われわれは最近，このような血管障害部位を特異的に造影できるMRI血管造影剤の開発を進めており，簡単なモデルではあるが，良い性能を有して

Yoshiki Katayama[1], Tatsuhiro Yamamoto[2], Hiroaki Shimokawa[3]
Department of Applied Chemistry, Faculty of Engineering, Kyushu University, Professor[1]
Department of Cardiovascular Medicine, Kyushu University Graduate School of Medical Sciences, Associate Professor[3]
MRI contrast agent that can recognize endothelium lesion
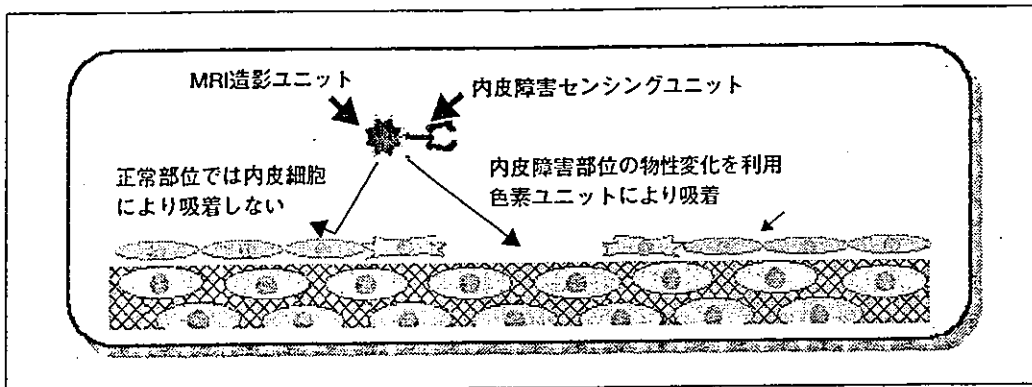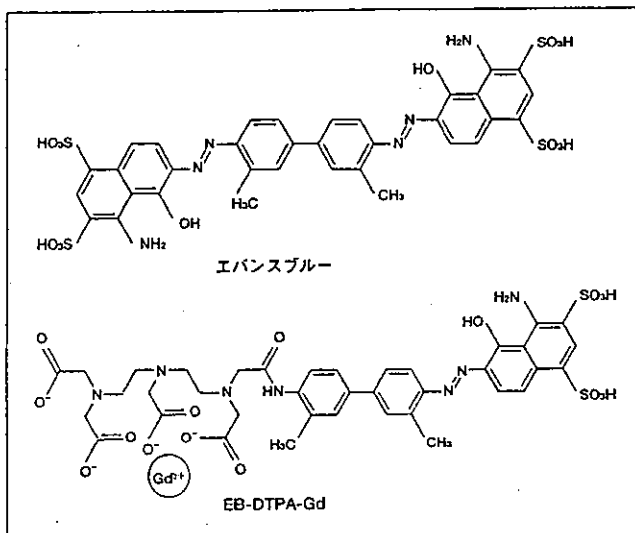E-mail : ykatalcm@mbox.nc.kyushu-u.ac.jp

図1　内皮障害部位認識型MRI造影剤の概念

図2　エバンスブルーと新規造影剤（EB-DTPA-Gd）の構造

いることを見出している。ここでは，その造影剤に関する設計と性能に関してご紹介する。

I. 血管障害部位特異的造影剤の設計

　ここで開発したのはMRI造影剤である。MRIは，各組織周辺の水分子の磁気による緩和現象の差を利用して組織をイメージングする手法である。体内において特定箇所を特異的にMRI造影する試みは，血管新生部位の造影として抗インテグリン抗体を連結したもの[1]，脳炎症部位に対して抗ICAM抗体を連結したもの[2] など種々の造影剤が報告されている。一方，血管障害部位を造影するためには，当該箇所を何らかの方法で認識しなくてはならない。例えば血栓を画像化するために抗フィブリン抗体やRGDペプチドを結合したものや[3,4]，MRI測定条件の設

定によりプラークを可視化する試みなどが報告されている[5]。

　ここで標的とするプラークや内皮障害部位は炎症箇所であるから，当然，E-セレクチンなどの標的分子に対する抗体や糖，ペプチドなどの結合分子を用いるのが通常の考え方である。しかしながら，例えば冠状動脈などでは非常に大きな血流量を有し，用いる造影剤は極めて大量に必要であるため，このような高価な生体分子を用いることは実用的観点からは困難である。また，実際に大量の血流にさらされた場合，その結合力あるいは結合速度が十分でなく，一度クランプにより血流を停止させて造影剤を結合させるという手法がとられる場合も多い。一方，血管が攣縮を起こす炎症箇所やバルーン障害箇所では，血管内面を覆う内皮細胞が傷害を受けており，これに伴う血管内面のマクロな物性変化を指標とすれば，新たな認識戦略が考えられる（図1）。

　この発想に基づき，われわれは単離したブタ大動脈片を展開し，その半分の領域の内皮細胞を物理的に傷害した系を用い，組織染色などで用いられる種々の有機色素をスクリーニングした。その結果，いくつかの構造を有するアゾ系の色素が，内皮が傷害された部位にのみ吸着し，正常内皮部位には吸着しないことを見出した。これらの色素のなかで，最もその性能に優れていたエバンスブルーを元に，図2のようなMRI造影剤（EB-DTPA-Gd）を設計した。この分子は，エバンスブルー類似骨格とMRI造影ユニットであるDTPA-Gd錯体を有している[6]。
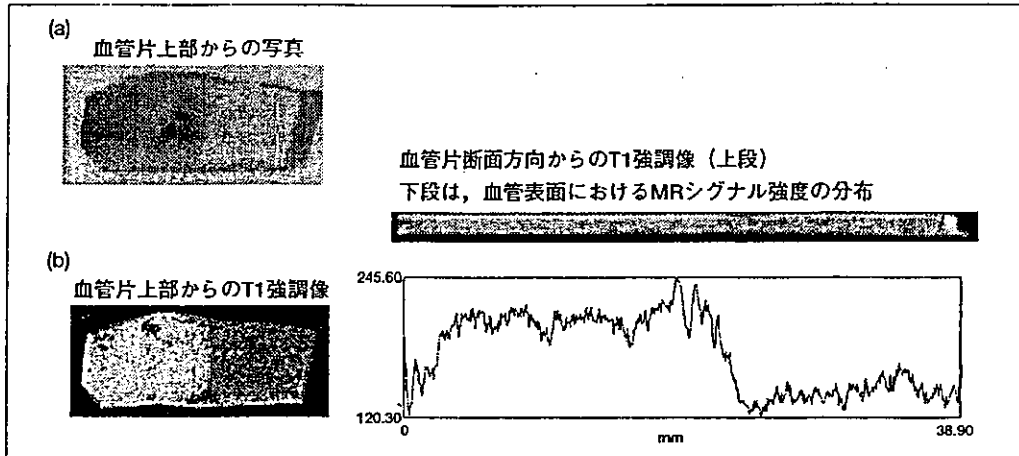
図3　摘出血管サンプルでの内皮剥離部位の造影結果

II. Gd錯体によるMRイメージングの原理

　ガドリニウムイオンはランタノイド系列に属し、核磁気共鳴測定時において周辺部の水分子プロトンに対し強力な緩和促進作用を有する。従って、当該イオンの存在箇所においては緩和時間が減少する。この緩和作用は、T1（縦緩和）に顕著に現れるため、これを画像化するのがMRI法におけるT1強調画像である。ガドリニウムイオンは、生体内においてカルシウムイオンなどと似た挙動を示すため、毒性を有する。DTPAは、強力なキレート剤であり、極めて強力にガドリニウムイオンを結合するため、その毒性は抑えられ、臨床試験でも安全性は確認されている。

III. 血管片を用いた内皮障害部位の検出

　合成したEB-DTPA-Gdを用いて、まず単離血管片を用いての内皮障害部位への造影剤の吸着を検討した。まず、ブタ大動脈を2〜3cmの長さに切断し、メスによりこれを展開して内皮面を露出させ、左半分の内皮を物理的に傷害した。これを10mMのEB-DTPA-GdあるいはDTPA-Gdの生理食塩水溶液に浸し、その後、生理食塩水で洗浄したところ、EB-DTPA-Gdは、内皮を傷害した部分にのみ選択的に吸着していることがわかった（図3a）。また、この血管片を生理食塩水に浸した状態でMRIでT1強調像を測定したところ、図3bのように、EB-

DTPA-Gdが吸着した標的内皮障害部位にシグナルが得られた。また、断面の像から、本造影剤は血管表面に限局していることも明らかとなった。造影剤が血管内に浸潤することは造影剤が長く体内にとどまることを意味し、好ましいことではないから、この結果は本化合物の造影剤としての用途に期待をもたせるものである。

　また、本造影剤の性質と構造の相関を調べるため、EB-DTPA-Gdから、ナフタレン部分を除去したDMBDTPA-Gdとさらにエバンスブルー関連骨格をすべて除去した通常のDTPA-Gdにより、同様に血管片での実験を行い、また、3者での血管断面の深さ方向のMRシグナル強度を計測した（図4）。その結果、EB-DTPA-Gdでは、分子は内皮剥離部位の表面のみに存在し、その下の細胞間マトリックス層や平滑筋層には全く存在しなかった。一方、DMBDTPA-Gdでは、いくぶん内皮剥離部位への優先的結合がみられるものの、分子は血管組織内部にまで浸潤し、平滑筋層を含む全体にシグナルがみられた。エバンスブルー骨格要素を全くもたないDTPA-Gdでは、当然のことながら全く血管への吸着はみられなかった。これらの事実より、血管内皮剥離部位への結合にはある程度の疎水性部分が必要であるが、疎水性が高いとそのまま組織内へ浸潤してしまうことがわかる。内皮剥離部位を認識しつつ、表面のみへの吸着を実現するには、エバンスブルーにみられるスルホン酸基のような極性基も同時に必要であることがわかる。元来、
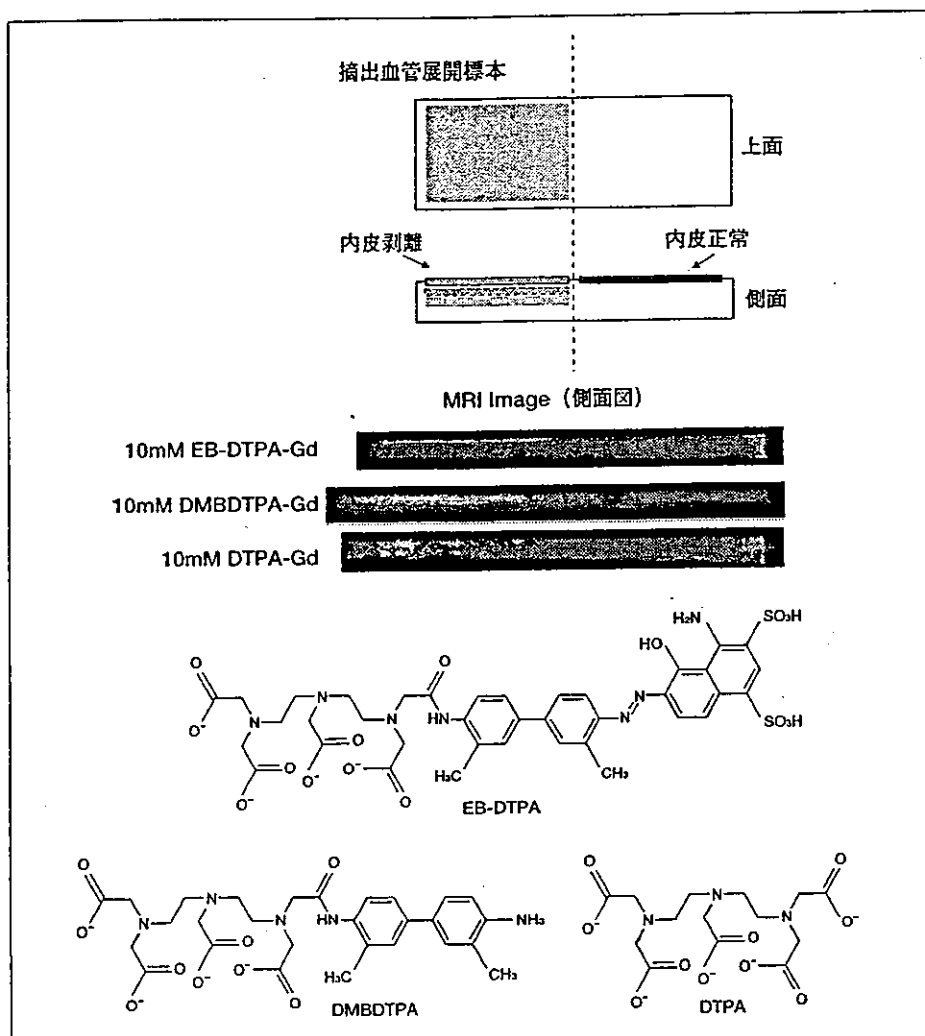
図4　造影剤の構造と血管への吸着能

このような色素は通常の組織では非常によく吸着する性質を有しているが，高度に水溶性の官能基が疎水環境にある組織内部に浸透することを抑制しているものと考えられる。また，内皮細胞層は，一般に血管への物質の無制限の透過を抑制するバリアとしても働いており，内皮が正常な部位ではこのような色素の吸着を許さないのであろう。

また，EB-DTPA-Gdに基づく内皮剥離部位でのMRIシグナル強度は，濃度依存性であり，数mM以上の濃度ではその強度増大は飽和したことから，使用濃度を10mMとしている。

エバンスブルーは，通常のタンパクへの吸着力も大きいと考えられる。特に，血管造影剤に適用した場合には，血液中のアルブミンなどへ吸着が大きい。実際，エバンスブルー自体は，静注により投与するとアルブミンと結合し，尿排泄されることが知られている。これを利用して，全血量の測定などを行う手法は古くからヒトにおいても適用されている。

EB-DTPA-Gdのアルブミンへの吸着が内皮障害部位への吸着を阻害する可能性を評価するために，同様の血管片を用いた実験で，生理食塩水ではなく血清を用いてMRI造影を試みた。その結果，生理食塩水中と同様の，標的部位におけるシグナル増強を認め，本造影剤が血液存在下でも妨害されることなく，標的部位に結合できることを確認した。

図5　造影剤静注後の両側頸動脈展開標本（*ex vivo*実験）

IV. *Ex vivo, in vivo*での評価

　EB-DTPA-Gdが摘出血管において，内皮障害部位特異的造影剤としての性能を有していることが明らかになったため，次にラットを用いて実際に静注したEB-DTPA-Gdが血管の内皮障害部位に結合できるのかを検討した。まず，大腿動脈からカテーテルを挿入し，バルーンにより左総頸動脈部分で内皮障害を作製し，次いで右頸静脈からEB-DTPA-Gdを10mM濃度で静注した。種々の時間が経過後，ラットを殺し両方の総頸動脈を摘出して展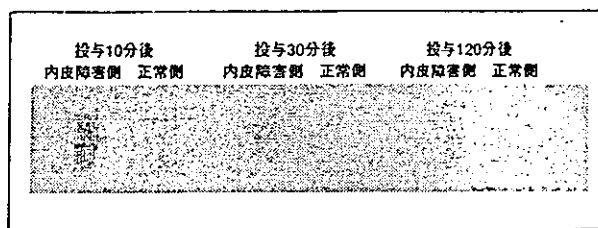開したところ，投与10分後でバルーン障害を施した左頸動脈でのみ造影剤の吸着が顕著にみられた（図5）。このことは，本造影剤が，体内の血流循環時においても，内皮障害部位に特異的に吸着できることを示している。また，内皮障害部位への吸着も時間とともに減少し，投与2時間後では，ほぼ正常血管と同レベルに戻った。すなわち，EB-DTPA-Gdは，実際に血管を造影できる程度の時間，標的部位に滞留する結合力を有しており，しかし，その結合は可逆的であり，血流により剝離し，ついには標的部位から除かれることを示しており，これも実際に造影剤として適用する場合には好ましい性質といえる。

　EB-DTPA-Gdの静注後のファーマコキネティクス（体内動態）も検討している。すなわち，投与後，30分と2時間の時点での各臓器を処理し，含まれるガドリニウムの量をICPにより定量したところ，本造影剤は各種臓器にはほとんど分配されず，血液と腎臓にのみ分配していた。この結果は，本造影剤が血液中を循環後，主として腎排泄され，その他の臓器への移行は無視できることを示している。データが未公表であるため詳細はご紹介できないが，これらの事実を踏まえ，実際に生きた

ラットでの血管障害モデルを用いた *in vivo* MRIにおいても，本造影剤が標的血管障害部位を特異的に造影できることも確かめており，EB-DTPA-Gdの実用性を支持している。

おわりに

　血管内皮障害を引き起こす炎症部位，特に動脈硬化に伴う不安定プラーク部位の特異的診断は，現在よい方法が存在しないが，もし可能になればその恩恵は非常に大きいものがある。今回開発した造影剤は，実際に静注により体内で内皮障害部位を特異的に診断できることが示されており，体内動態，標的部位への結合性，その後の滞留性などにほぼ理想的な性質を有している。実用性をさらに検証していくことで，さらに分子の改良を含めての最適化が必要となることは考えられるが，非常に興味深い基本構造であるといえる。今後は，動脈硬化モデルや大型動物を用いての検討を加え，実用性を追求していきたいと考えている。また，それと同時に，本造影剤の標的部位への結合のメカニズムの解明も急務である。内皮障害血管部位での本造影剤の結合標的分子の探索を進めているところである。

参考文献
1) Anderson SA, Rader RK, et al : Magn Reson Med 44, 433-439, 2000.
2) Sipkins DA, Gijbels K, et al : J Neuroimmunol 104, 1-9, 2000.
3) Flacke S, Fischer S, et al : Circulation 104, 1280-1285, 2001.
4) Johansson LO, Bjomerud A, et al : J Magn Reson Imaging 13, 615-618, 2001.
5) Fayad ZA, Fuster V : Circ Res 89, 305-316, 2001.
6) Yamamoto T, Ikuta K, et al : Anal Sci, in press.

著者プロフィール
片山佳樹：
1987年　九州大学大学院工学研究科博士課程修了（工学博士）
　　　　（株）同仁化学研究所入社
1988年　同研究部主任研究員
1990年　英国王立医学研究所客員研究員（～1992年）
1994年　（株）同仁化学研究所研究部チーフ
1996年　九州大学工学研究院助教授
1999年　科学技術振興事業団PRESTO研究員兼任（～2002年）
2003年　九州大学工学研究院教授
　　　　科学技術振興機構CREST研究代表兼務
　　　　現在に至る

Photochemical Study of [3₃](1,3,5)Cyclophane and Emission Spectral Properties of [3ₙ]Cyclophanes (*n* = 2–6)

Rika Nogita, Kumi Matohara, Minoru Yamaji, Takuma Oda,
Youichi Sakamoto, Tsutomu Kumagai, Chultack Lim,
Mikio Yasutake, Tetsuro Shimo, Charles W. Jefford, and
Teruo Shinmyozu

Contribution from Institute for Materials Chemistry and Engineering
(IMCE) and Department of Molecular Chemistry, Graduate School of
Sciences, Kyushu University, Hakozaki 6-10-1, Fukuoka 812-8581,
Japan, Department of Chemistry, Gunma University, Kiryu,
Gunma 376-8515, Japan, Institute for Molecular Science, Myodaiji,
Okazaki 444-8585, Japan, Department of Chemistry, Graduate School
of Science, Tohoku University, Sendai 980-8577, Japan, and
Department of Applied Chemistry and Chemical Engineering,
Faculty of Engineering, Kagoshima University, Korimoto 1-21-40,
Kagoshima 890-0065, Japan, Departement de
Chimie Organique Section de Chimie 30, Universite de Geneva,
quai Ernest Ansermet CH-1211 Geneva 4, Switzerland

Photochemical Study of [3₃](1,3,5)Cyclophane and Emission Spectral Properties of [3$_n$]Cyclophanes ($n = 2-6$)

Rika Nogita,[†,‡] Kumi Matohara,[†,‡] Minoru Yamaji,[§] Takuma Oda,[†,‡]
Youichi Sakamoto,[#] Tsutomu Kumagai,[‖] Chultack Lim,[†] Mikio Yasutake,[†,‡]
Tetsuro Shimo,[⊥] Charles W. Jefford,[¶] and Teruo Shinmyozu*,[†]

*Contribution from Institute for Materials Chemistry and Engineering (IMCE)
and Department of Molecular Chemistry, Graduate School of Sciences, Kyushu University,
Hakozaki 6-10-1, Fukuoka 812-8581, Japan, Department of Chemistry, Gunma University,
Kiryu, Gunma 376-8515, Japan, Institute for Molecular Science, Myodaiji,
Okazaki 444-8585, Japan, Department of Chemistry, Graduate School of Science,
Tohoku University, Sendai 980-8577, Japan, and Department of Applied Chemistry and
Chemical Engineering, Faculty of Engineering, Kagoshima University, Korimoto 1-21-40,
Kagoshima 890-0065, Japan, Departement de Chimie Organique Section de Chimie 30,
Universite de Geneva, quai Ernest Ansermet CH-1211 Geneva 4, Switzerland*

Received January 16, 2003; E-mail: shinmyo@ms.ifoc.kyushu-u.ac.jp

Abstract: The photochemical reaction of [3₃](1,3,5)cyclophane 2, which is a photoprecursor for the formation of propella[3₃]prismane 18, was studied using a sterilizing lamp (254 nm). Upon photolysis in dry and wet CH_2Cl_2 or MeOH in the presence of 2 mol/L aqueous HCl solution, the cyclophane 2 afforded novel cage compounds comprised of new skeletons, tetracyclo[6.3.1.0.²,⁷0⁴,¹¹]dodeca-5,9-diene 43, hexacyclo-[6.4.0.0.²,⁶0.⁴,¹¹0.⁵,¹⁰0⁹,¹²]dodecane 44, and pentacyclo[6.4.0.0.²,⁶0.⁴,¹¹0⁵,¹⁰]dodecane 45. All of these products were confirmed by the X-ray structural analyses. A possible mechanism for the formation of these photoproducts via the hexaprismane derivative 18 is proposed. The photophysical properties in the excited state of the [3$_n$]cyclophanes ([3$_n$]CP, $n = 2-6$) were investigated by measuring the emission spectra and determining the quantum yields and lifetimes of the fluorescence. All [3$_n$]CPs show excimeric fluorescence without a monomeric one. The lifetime of the excimer fluorescence becomes gradually longer with the increasing number of the trimethylene bridges. The [3$_n$]CPs also shows excimeric phosphorescence spectra without vibrational structures for $n = 2$, 4, and 5, while phosphorescence is absent for $n = 3$ and 6. With an increase in symmetry of the benzene skeleton in the [3₃]- and [3₆]CPs, the probability of the radiation (phosphorescence) process from the lowest triplet state may drastically decrease.

1. Introduction

All members of the [3$_n$]cyclophanes ([3$_n$]CPs, $n = 2-6$) are available today[2,3] because of our efforts aimed at the synthesis of [3₆](1,2,3,4,5,6)CP 6, [3]superphane, with bridges longer, by one carbon unit, than that of [2₆](1,2,3,4,5,6)CP (superphane) 7 by Boekelheide et al.[4] and Hopf et al. (Figure 1).[5] Elongation of the bridge causes the cyclophane structure to be increasingly
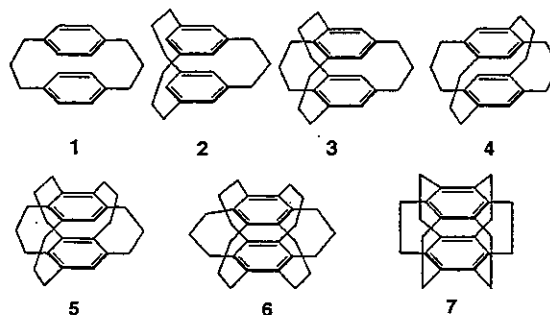
† Institute for Materials Chemistry and Engineering (IMCE), Kyushu University.

‡ Department of Molecular Chemistry, Graduate School of Sciences, Kyushu University.

§ Department of Chemistry, Gunma University.

Institute for Molecular Science.

‖ Department of Chemistry, Graduate School of Science, Tohoku University.

⊥ Department of Applied Chemistry and Chemical Engineering, Faculty of Engineering, Kagoshima University.

¶ Department de Chimie Organique Section de Chimie 30, Universite de Geneva.

(1) Multibridged [3n]cyclophanes, part 17.
(2) (a) Sakamoto, Y.; Miyoshi, N.; Shinmyozu, T. *Angew. Chem., Int. Ed. Engl.* **1996**, *35*, 549–550. (b) Sakamoto, Y.; Miyoshi, N.; Hirakida, M.; Kusumoto, S.; Kawase, H.; Rudzinski, J. M.; Shinmyozu, T. *J. Am. Chem. Soc.* **1996**, *118*, 12267–12275. (c) Sakamoto, Y.; Shinmyozu, T. *Recent Res. Dev. Pure Appl. Chem.* **1998**, *2*, 371–399.

Figure 1. [3$_n$]Cyclophanes ($n = 2-6$) 1–6 and superphane 7.

strain-free and more flexible compared with the corresponding [2$_n$]CP series. As a result, the [3$_n$]CPs show much stronger

(3) (a) Meno, T.; Sako, K.; Suenaga, M.; Mouri, M.; Shinmyozu, T.; Inazu, T.; Takemura, H.; *Can. J. Chem.* **1990**, *68*, 440–445. (b) Shinmyozu, T.; Hirakida, M.; Kusumoto, S.; Tomonou, M.; Inazu, T.; Rudzinski, J. M. *Chem. Lett.* **1994**, 669–672. (c) Sentou, W.; Satou, T.; Yasutake, M.; Lim, C.; Sakamoto, Y.; Itoh, T.; Shinmyozu, T. *Eur. J. Org. Chem.* **1999**, 1223–1231.
(4) (a) Sekine, Y.; Brown, M.; Boekelheide, V. *J. Am. Chem. Soc.* **1979**, *101*, 3126–3127. (b) Sekine, Y.; Boekelheide, V. *J. Am. Chem. Soc.* **1981**, *103*, 1777–1785.
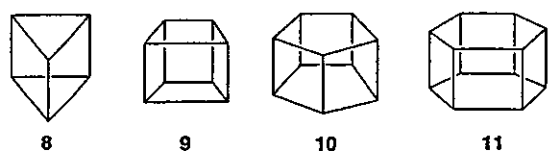
Figure 2. Prismane family.

π-electron donating ability than the corresponding [2ₙ]CPs.[2,6] We have already reported the synthetic methods of the [3ₙ]CPs and their structural properties in solution[2] as well as in the solid state.[6] Our next subject to be solved in this field is the synthesis of propella[3ₙ]prismanes via photochemical reaction of the [3ₙ]-CPs.[7,8]

Prismanes constitute an infinite family of (CH)ₙ polyhedra[9] that chemists find esthetically appealing because of their molecular architecture (Figure 2). Notwithstanding their structural regularity, many years of effort were needed before the first three members, prismane **8**,[10] cubane **9**,[11] and pentaprismane **10**,[12] could be successfully synthesized. Recently, attention has been focused on the challenging objective of constructing the higher prismanes, in particular, hexaprismane **11**. Many diverse synthetic strategies have been developed, and significant progress toward the synthesis of hexaprismane **11** has been made.[13–16] For example, synthesized secohexaprismane, in which only one C—C bond is missing from hexaprismane **11**.[15] However, **11** has eluded synthesis so far.

Pentacyclo[6.4.0.0.²'⁷0.³'¹²0⁶'⁹]dodeca-4,10-diene **12**, an attractive and logical precursor, could not be photochemically converted to **11** (Scheme 1).[17] This result might have been anticipated because the related olefin, *syn*-tricyclo[4.2.0.0²'⁵]octa-3,7-diene **13** failed to give cubane **9** via [2+2]photocyclization.[18] However, the photochemical formation of propella[3₄]prismane **15** from diene **14** is indicative that attaching trimethylene bridges

Scheme 1. Intramolecular [2+2] Photochemical Reactions
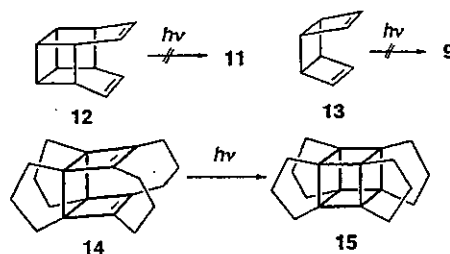
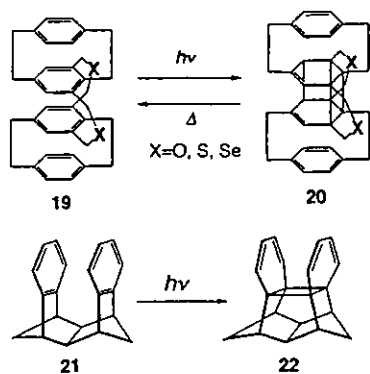**Scheme 2.** Expected Photochemical Reactions
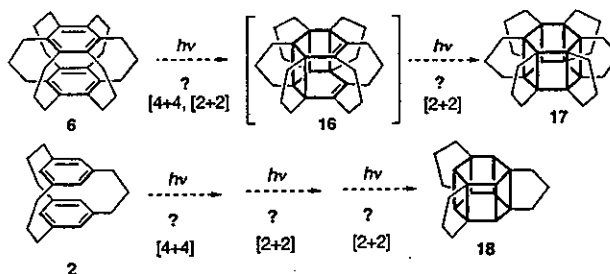
to the basic skeleton may enable [2+2]photocyclization leading to the prismane skeletons (Scheme 1).[19] These findings have been rationalized in terms of the order of the frontier molecular orbitals which are largely affected by through-bond interactions.[20–23] Moreover, on the basis of Frontier MO consideration, it was predicted that [3]superphane **6** would give the hexaprismane derivative **17** on irradiation.[20] It could be argued that three trimethylene bridges would be just as effective as six making the [3₃]CP **2** a likely candidate for conversion to the triply bridged hexaprismane **18** (Scheme 2). Before putting this prediction to the test, we decided to first investigate the photochemical behavior of less substituted **2** with the aim of optimizing the reaction conditions. We now describe experiments with **2**,[3a,24] the lower homologue of **6**, which has the advantage of being available in large quantities.

Benzene is very stable to photochemical reaction so that the photodimer of benzene has hardly been characterized except for a few examples, whereas the photodimer of condensed aromatics such as naphthalene and anthracene has been reported.[25] Misumi et al. first reported the novel photodimerization of benzene rings incorporated into *syn*-quadruple-layered dihetera-cyclophane **19** and concluded that the photodimerization is affected by the face-to-face stacking of two fairly strained benzene rings, as well as the substituted positions of four bridges at the inner benzenes and that the outer benzene rings are required for an increase in thermal stability of the photoisomers **20** but not for photodimerization (Scheme 3).[26] Prinzbach et al. reported a second example of the photodimerization of benzene rings in a rigid polycyclic cage, the [6+6] photocyclization between two benzene rings in solution (**21** to **22**).[27] They

(5) El-tamany, S.; Hopf, H.; *Chem. Ber.* **1983**, *116*, 1682−1685.
(6) (a) Yasutake, M.; Koga, T.; Sakamoto, Y.; Komatsu, S.; Zhou, M.; Sako, K.; Tatemitsu, H.; Onaka, S.; Aso, Y.; Inoue, S.; Shinmyozu, T. *J. Am. Chem. Soc.* **2002**, 10136−10145. (b) Yasutake, M.; Araki, M.; Zhou, M.; Nogita, R.; Shinmyozu, T. *Eur. J. Org. Chem.* **2003**, 1343−1351. (c) Yasutake, M.; Koga, T.; Lim, C.; Zhou, M.; Matsuda-Sentou, W.; Satou, T.; Shinmyozu, T. In *Cyclophane Chemistry for the 21st Century*; Takemura, H., Ed.; Research Signpost: Kerana, India, 2002, pp 265−300.
(7) (a) Sakamoto, Y.; Kumagai, T.; Matohara, K.; Lim, C.; Shinmyozu, T. *Tetrahedron Lett.* **1999**, *40*, 919−922. (b) Matohara, K.; Lim, C.; Yasutake, M.; Nogita, R.; Koga, T.; Sakamoto, Y.; Shinmyozu, T. *Tetrahedron Lett.* **2000**, *41*, 6803−6807.
(8) (a) Lim, C.; Yasutake, M.; Shinmyozu, T. *Angew. Chem., Int. Ed. Engl.* **2000**, *39*, 578−580. (b) Lim, C.; Yasutake, M.; Shinmyozu, T. *Tetrahedron Lett.* **1999**, *40*, 6781−6784.
(9) For recent reviews, see. (a) Shinmyozu, T.; Nogita, R.; Akita, M.; Lim, C. In *CRC Handbook of Organic Photochemistry and Photobiology*, 2nd edition; Horspool, W., Lench, F., Eds.; CRC Press: USA, 2003, 23−1−23−11. (b) Dodziuk, H. In *Topics in Stereochemistry*; Eliel, E. L., Wilen, S. H., Eds.; John Wiley & Sons: New York, 1994; Vol. 21. (c) Dodziuk, H. Modern Conformational Analysis, VCH Publishers: 1995. (d) Forman, M. A. *Org. Prep. Proced. Int.* **1994**, *26*, 291−320.
(10) Katz, T. J.; Acton, N. *J. Am. Chem. Soc.* **1973**, *86*, 2035−2037.
(11) (a) Eaton, P. E.; Cole, Jr. T. W. *J. Am. Chem. Soc.* **1964**. *86*, 962−963. (b) Eaton, P. E.; Cole, Jr. T. W. *J. Am. Chem. Soc.* **1964**, *86*, 3157−3158. (c) Eaton, P. E. *Angew. Chem., Int. Ed. Engl.* **1992**, *31*, 1421−1436.
(12) (a) Eaton, P. E.; Or, Y. S.; Branca, S. J. *J. Am. Chem. Soc.* **1981**, *103*, 2134−2136. (b) Eaton, P. E.; Or, Y. S.; Branca, S. J.; Ravi Shanker, B. K. *Tetrahedron* **1986**, *42*, 1621−1631.
(13) Eaton, P. E.; Chakraborty, U. R. *J. Am. Chem. Soc.* **1978**, *100*, 3634−3635.
(14) (a)Mehta, G.; Padma, S. *J. Am. Chem. Soc.* **1987**, *109*, 7230−7237. (b) Mehta, G.; Padma, S. *Tetrahedron* **1991**, *47*, 7807−7820.
(15) (a) Mehta, G.; Padma, S. *J. Am. Chem. Soc.* **1987**, *109*, 2212−2213. (b) Mehta, G.; Padma, S. *Tetrahedron Lett.* **1991**, *47*, 7783−7806.
(16) (a) Dailey, W. P.; Golobish, T. D. *Tetrahedron* **1996**, *37*, 3239−3242. (b) Chou, T —C.; Lin, G.-H.; Yeh, Y.-L.; Lin, K.-J. *J. Chinese Chem. Soc.* **1997**, *44*, 477−493.
(17) Yang, N. C.; Homer, M. G. *Tetrahedron Lett.* **1986**, *27*, 543−546.
(18) Iwamura, H.; Morino, K.; Kihara, H. *Chem. Lett.* **1973**, 457−460.

(19) (a) Gleiter, R.; Karcher, M. *Angew. Chem. Int. Ed. Engl.* **1988**, *27*, 840−841. (b) Brand, S.; Gleiter, R. *Tetrahedron Lett.* **1997**, *38*, 2939−2942. (c) Gleiter, R.; Brand, S. *Chem. Eur. J.* **1998**, *4*, 2532−2538.
(20) Cha, O. J.; Osawa, E.; Park, S. *J. Mol. Struct.* **1993**, *300*, 73−81.
(21) Dailey, W. P. *Tetrahedron Lett.* **1987**, *28*, 5787−5990.
(22) Disch, R. L.; Schulman, J. M. *J. Am. Chem. Soc.* **1988**, *110*, 2102−2105.
(23) Engelke R. *J. Am. Chem. Soc.* **1986**, *108*, 5799−5803 and references therein.
(24) Hubert, A. J. *J. Chem. Soc. C* **1967**, 6−10.
(25) Chandross, E. A.; Dempster, C. J. *J. Am. Chem. Soc.* **1970**, 704−706.
(26) (a) Higuchi, H.; Takatsu, K.; Otsubo, T.; Sakata, Y.; Misumi, S. *Tetrahedron Lett.* **1982**, *23*, 671−672. (b) Higuchi, H.; Kobayashi, E.; Sakata, Y.; Misumi, S. *Tetrahedron* **1986**, 42, 1731−1739.
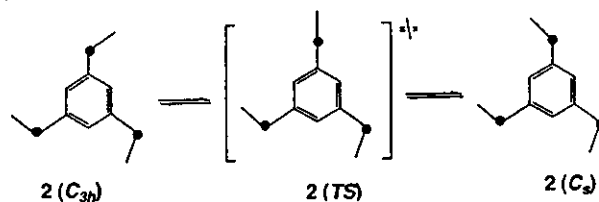
Scheme 3. Novel Photodimerizations of Benzene Rings in the
Syn-Quadruple-Layered Diheteracyclophane 19 and 21

Scheme 4. Bridge Flipping Process and Two Stable Conformers
(C_{3h} and C_s) of [3₃](1,3,5)Cyclophane 2

proposed a synthetic route of the doubly birdcage-annelated hexaprismane derivatives via the [2+2] photocyclization.[28] Thus, a limited number of this type [2+2] photocyclization between two benzene rings has been reported so far. In our photochemical approach to the construction of propella[3ₙ]prismanes, the [3ₙ]-CPs (n = 3–6), in which two benzene rings are completely stacked at 3.0–3.2 Å transannular distances, are used for the precursors.[6a]

The [3ₙ]CPs are very useful chromophores for the study of the singlet and triplet excimer states.[29] An investigation of the excimeric states of aromatic compounds in intramolecular and intermolecular systems has been reported.[25,29a] The unique spectroscopic and photochemical properties of [2.2]metacyclophane and related compounds,[30] fluorene,[31] naphthalene derivatives,[32,33] and anthracene derivatives[34] with transannular π-electronic interaction have been extensively studied as benzene dimer models.[35] Fluorescence and phosphorescence from an excimer, a transient singlet and a triplet dimer formed by the association of electronically excited and unexcited molecules, have been observed for a number of aromatic hydrocarbons in liquid solution, pure liquid, and the crystalline state. However, only in the case of benzene, observation and definite conclusion have not been drawn because of the difficulty of its measure-

ments except for gas-phase measurement. The [3ₙ]CPs may elucidate this problem by behaving as a benzene dimer in the excited state due to their structural character, where the two benzene ring are completely stacked face to face by trimethylene chains. Furthermore, the [3ₙ]CPs should show excimer emission efficiently rather than the [2ₙ]CPs on the basis of a statistical rule known as Hirayama's n = 3 rule.[36]

We wish to report here a photochemical study of [3₃]CP 2 directed toward the synthesis of the first hexaprismane derivative, propella[3₃]prismane 18, and the emission spectral properties of the [3ₙ]CPs (n = 2–6) as fundamental information on the excited states.
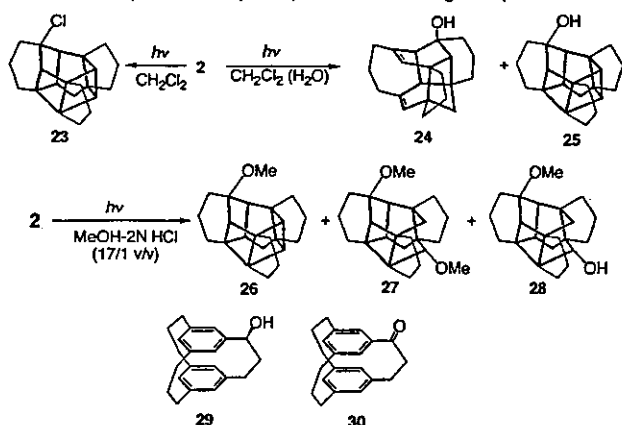
2. Results and Discussion

The precursor of the photochemical reaction, [3₃]CP 2, was prepared by the TosMIC coupling method as previously reported.[3a] Two conformers having C_{3h} and C_s symmetries are observed in the ¹H NMR spectrum of 2,2,11,11,20,20-hexadeuterated 2 in CD_2Cl_2, and 2 (C_S) is more stable than 2 (C_{3h}) by 0.4 kcal/mol. The energy barrier for the bridge flipping process is 12.4 kcal/mol (T_c = −7 °C) (Scheme 4),[3a] and the value is slightly higher than those of [3₂](1,3)-[37,38] and [3₂](1,4)-CPs.[39,40] The Density Functional calculations (B3LYP) estimated that the transition state 2 (TS) connecting the C_{3h} and the C_s conformers has only one flat bridge whose dihedral angle is calculated to be 180.0°, and one of three bridges can change its conformation independently without the influence of other bridges.[41] In the solid state, 2 takes the C_s conformation and the benzene rings are completely stacked with the transannular distance being 3.08–3.24 Å.[6a]

2.1. Photochemical Reaction of [3₃](1,3,5)Cyclophane 2.
Irradiation of 2 by a sterilizing lamp (λ = 254 nm) in cyclohexane, MeOH, or benzene left 2 intact, while causing some of the usual polymerization. However, two types of products were formed when CH_2Cl_2 was used as a solvent.[7] A dry CH_2Cl_2 solution of 2 (4.90 × 10⁻³ mol/L) in a quartz vessel

(27) (a) Prinzbach, H., Sedelmeier, G.; Kruger, C.; Goddart, R.; Martin, H. D.; Gleiter, R. *Angew. Chem., Int. Ed. Eng.* **1978**, *42*, 1731–1739. (b) Fessner, W. D.; Prinzbach, H. *Tetrahedron Lett.* **1983**, *24*, 5857–5860. (c) Prinzbach, H.; Sedelmeier, G.; Krüger, C.; Goddard, R.; Martin, H. D.; Gleiter, R. *Angew. Chem. Int. Ed. Engl.* **1978**, *17*, 271–272. (d) Wollenweber, M.; Hunkler, D.; Keller, M.; Knothe, L.; Prinzbach, *Bull. Soc. Chim. Fr.* **1993**, *130*, 32–57.
(28) Wollenweber, M.; Etzkorn, M.; Reinbold, J.; Wahl, F.; Voss, T.; Melder, J. P.; Grund, C.; Pinkos, R.; Hunkler, D.; Keller, M.; Wörth, J.; Knothe, L.; Prinzbach, H., *Eur. J. Org. Chem.* **2000**, 3855–3886.
(29) (a) Lim, E. C. *Acc. Chem. Res.* **1987**, *20*, 8–17. (b) Saigusa, H.; Lim, E. C. *Acc. Chem. Res.* **1996**, *29*, 171–178.
(30) (a) Shizuka, H.; Ogiwara, T.; Morita, T. *Bull. Chem. Soc. Jpn.* **1975**, *48*, 3385–3386. (b) Ishikawa, S.; Nakamura, J.; Iwata, S.; Sumitani, M.; Nagakura, S.; Sakata, Y.; Misumi, S. *Bull. Chem. Soc. Jpn.* **1979**, *52*, 1346–1350. (c) Kovac, B.; Mohraz, M.; Heilbronner, E.; Boekelhide, V.; Hopf, H. *J. Am. Chem. Soc.* **1980**, *102*, 4314–4324. (d) Dewhirst, K. C.; Cram, D. J. *J. Am. Chem. Soc.* **1958**. 3115–3125.
(31) (a) Saigusa, H.; Itoh, M. *J. Phys. Chem.* **1985**, *89*, 5486-5488. (b) Rani, S. A.; Sobhanadri, J.; Prasada Rao, T. A. *J. Photochem. Photobio. A: Chem.* **1996**, *94*, 1–5.
(32) (a) Yamaji, M.; Tsukada, H.; Nishimura, J.; Shizuka, H.; Tobita, S., *Chem. Phys. Lett.*. **2002**, *357*, 137–142. (b) Yamaji, M.; Shima, K.; Nishimura, J.; Shizuka, H.; *J. Chem. Soc., Faraday Trans.* **93**. 1065–1070. **1997**.
(33) (a) Nakamura, Y.; Fujii, T.; Nishimura. J. *Tetrahedron Lett.* **2000**, *41*, 1419–1423. (b) Nakamura, Y.; Kaneko, M.; Yamanaka, N.; Tani, K.; Nishimura, J. *Tetrahedron Lett.* **1999**, *40*, 4693–4696.
(34) Kaupp, G., *Angew. Chem., Int. Ed. Engl.* **1972**, *11*, 313–314.
(35) (a) Langridge-Smith, P. R. R.; Brumbaugh, V. D.; Haynman, A. C.; Levy, H. D. *J. Phys. Chem.* **1981**, *85*, 3742–3746. (b) Hopkins, J. B.; Power, D. E.; Smalley, R. E. *J. Phys. Chem.* **1981**, *85*, 3739–3742. (b) Gonzalez, C.; Lim, E. C. *J. Phys. Chem. A* **2001**, *105*, 1904–1908.

(36) Hirayama, F. *J. Chem. Phys.* **1965**, *42*, 3163–3171.
(37) Semmelhack, M. F.; Harrison, J. J.; Young, D. C.; Gutiérrez, A.; Rafii, S.; Clardy, J. J. *J. Am. Chem. Soc.* **1985**, *107*, 7508–7514.
(38) (a) Sako, K.; Hirakawa, T.; Fujimoto, N.; Shinmyozu, T.; Inazu, T.; Horimoto, H. *Tetrahedron Lett.* **1988**, *29*, 6275–6278. (b) Sako, K.; Shinmyozu, T.; Takemura, H.; Suenaga, M.; Inazu, T. *J. Org. Chem.* **1992**, *57*, 6536–6541. (c) Shinmyozu, T.; Hirakawa, T.; Wen, G.; Osada, S.; Takemura, H.; Sako, K.; Rudzinski, J. M. *Liebigs Ann.* **1996**, 205–210. (d) Sako, K.; Tatemitsu, H.; Onaka, S.; Takemura, H.; Osada, S.; Wen, G.; Rudzinski, J. M.; Shinmyozu, T. *Liebigs Ann.* **1996**, 1645–1649. (e) Takemura, H.; Kariyazono, H.; Kon, N.; Tani, K.; Sako, K.; Shinmyozu, T.; Inazu, T. *J. Org. Chem.* **1999**, *64*, 9077–9079. (f) Wen, G.; Matsuda-Sentou, W.; Sameshima, K.; Yasutake, M.; Noda, D.; Lim, C.; Satou, T.; Takemura, H.; Sako, K.; Tatemitsu, H.; Inazu, T.; Shinmyozu, T. submitted to *J. Am. Chem. Soc.* (g) Satou, T.; Shinmyozu, T. *J. Chem. Soc., Perkin Trans. 2* **2002**, 393–397.
(39) Anet, F. A. L.; Brown, M. A. *J. Am. Chem. Soc.* **1969**, *91*, 2389–2391.
(40) Sako, K.; Meno, T.; Takemura, H.; Shinmyozu, T.; Inazu, T. *Chem. Ber.* **1990**, *123*, 639–642.
(41) Hori, K.; Sentou, W.; Shinmyozu, T. *Tetrahedron Lett.* **1997**, *38*, 8955–8958.

Scheme 5. Photochemical Reaction of [3₃](1,3,5)Cyclophane **2** in Dry CH₂Cl₂ or Wet CH₂Cl₂ (upper) and in MeOH in the Presence of 2 mol/L Aqueous HCl (lower) under Sterilizing Lamp Irradiation

Figure 3. ORTEP drawings of the photoproduct **24** (−170 °C) (A) and its skeleton (B). Selected bond length (Å): C1−C2 1.543(3), C2−C3 1.521-(3), C3−C4 1.340(3), C4−C5 1.515 (3) C5−C6 1.563(3), C6−C1 1.538-(3), C7−C8 1.576(3), C8−C9 1.524(3), C9−C10 1.337(3), C10−C11 1.497(3), C11−C12 1.546(3), C2−C8 1.602(3), C5−C11 1.649(3), C12−C7 1.538(3).

was irradiated by a sterilizing lamp for 2.5 h at room temperature under Ar. Separation of the reaction mixture by silica gel column chromatography with hexane afforded a new cage compound, the bridged hexacyclic chlorododecane **23** (5.3%) and the recovery of the starting compound **2** (40%) (Scheme 5). The structure of **23** was first proposed from the molecular formula, NMR data [the distortionless enhancement by polarization transfer (DEPT) spectrum and the ¹H-¹³C correlation spectroscopy], elemental analysis, and mass spectral data (FABMS: m/z = 311 [M⁺ − 1]). Furthermore, the structure was confirmed by the fact that its ¹H- and ¹³C NMR data are quite similar to those of the alcohol **25** with the same structure as described below.[7a]

Irradiation of **2** under the same conditions as before, while in a CH₂Cl₂ solution saturated with water (1.45 × 10⁻² mol/L) for 2.5 h under Ar, followed by separation by column chromatography (SiO₂, hexane:AcOEt, 10:1), gave, in addition to **2** (18%), two photoproducts. The ¹H- and ¹³C NMR spectra of **25** are similar to those of **23**, suggesting that the two molecules have the same structure. The structure of the polycyclic olefin **24** was identified on the basis of the NMR data (¹H- and ¹³C NMR, DEPT spectrum), elemental analysis, mass spectral data (FABMS: m/z = 294 [M⁺]), and finally by X-ray structural analysis. The novel polycyclic diolefin **24** is composed of one cyclooctadiene, one cycloheptane, one cyclohexane, and two cyclohexene rings, which originate from the benzene rings, and three cyclopentanes (Figure 3A). The C3−C4 [1.340(3) Å] and C9−C10 [1.337(3) Å] bonds are double bonds. The upper and lower cyclohexenes are connected at three positions, C2−C8, C6−C7, and C5−C11 (Figure 3B). The upper cyclohexene ring takes the strained half-chair form of the cyclohexene [the dihedral angles of C2−C3−C4−C5 is −10.8(2)°]. To release this deviation, the bond lengths of C2−C8 [1.602(3) Å] and C5−C11 [1.649(3) Å] are abnormally long compared with the RHF/6-31G* optimized C−C bond length (1.552 Å) of a cyclopentane. The crystal packing diagram of **24** is shown in Figure S1 in the Supporting Information, and the crystal data of **24** as well as those of other photoproducts **25**, **27**, **28**, and **31**, which will be mentioned hereafter, are summarized in Table S1 in the Supporting Information.

The structure of the cage compound **25** was determined by X-ray structural analysis (−170 °C) (Figure 4A). Compound **25** has the highest strain energy among the identified photo-
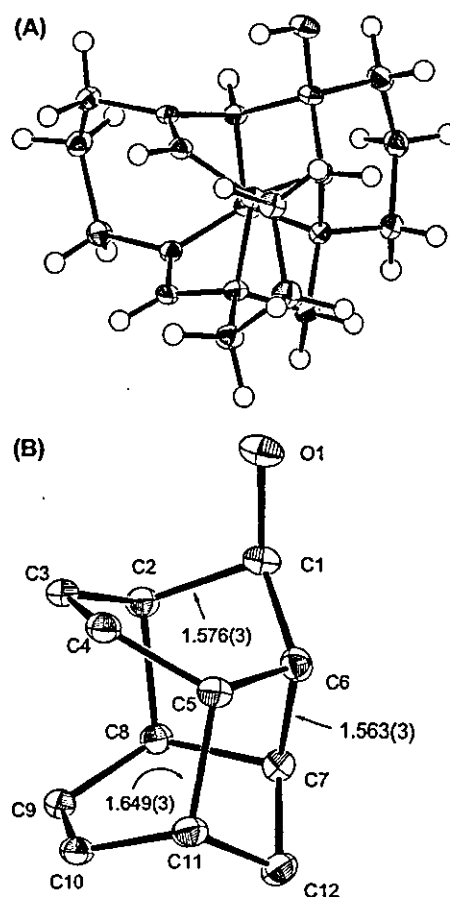
products because it has three consecutive cyclobutane rings. The skeleton of **25** is composed of the three consecutive cyclobutane rings and two cyclopentane rings. The cyclobutane rings are not square but are rectangular, and the magnitude of the deviation is significant in the central cyclobutane ring. The C3−C12 and C4−C13 bonds are significantly longer than other C−C bonds of the cyclobutane rings. However, a detailed discussion of the C−C bond lengths cannot be provided at the present stage because of the insufficient quality of the X-ray data. A more precise X-ray analysis of **25** is in progress. The central cyclobutane ring, therefore, is expected to be more reactive than the terminal rings, and in fact, the more strained central cyclobutane ring undergoes protonation in preference to the terminal rings as described later.

To reveal the photochemical reaction mechanism, the photolysis of **2** in acidic and basic conditions was examined. A CD₃OD or CD₃CN solution of **2** (2.71 × 10⁻² mol/L) containing 2 mol/L aqueous HCl solution (one drop) in a quartz NMR tube was irradiated with a sterilizing lamp for 2.5 h at room temperature under Ar, and the reaction was monitored by the ¹H NMR spectra. The reaction proceeded in acidic conditions, whereas the reaction in CD₂Cl₂ in the presence of triethylamine did not proceed. Because the reaction afforded photoproducts only in CH₂Cl₂ or CD₃CN and CD₃OD in the presence of HCl, the heavy atom effect on product formation was examined.
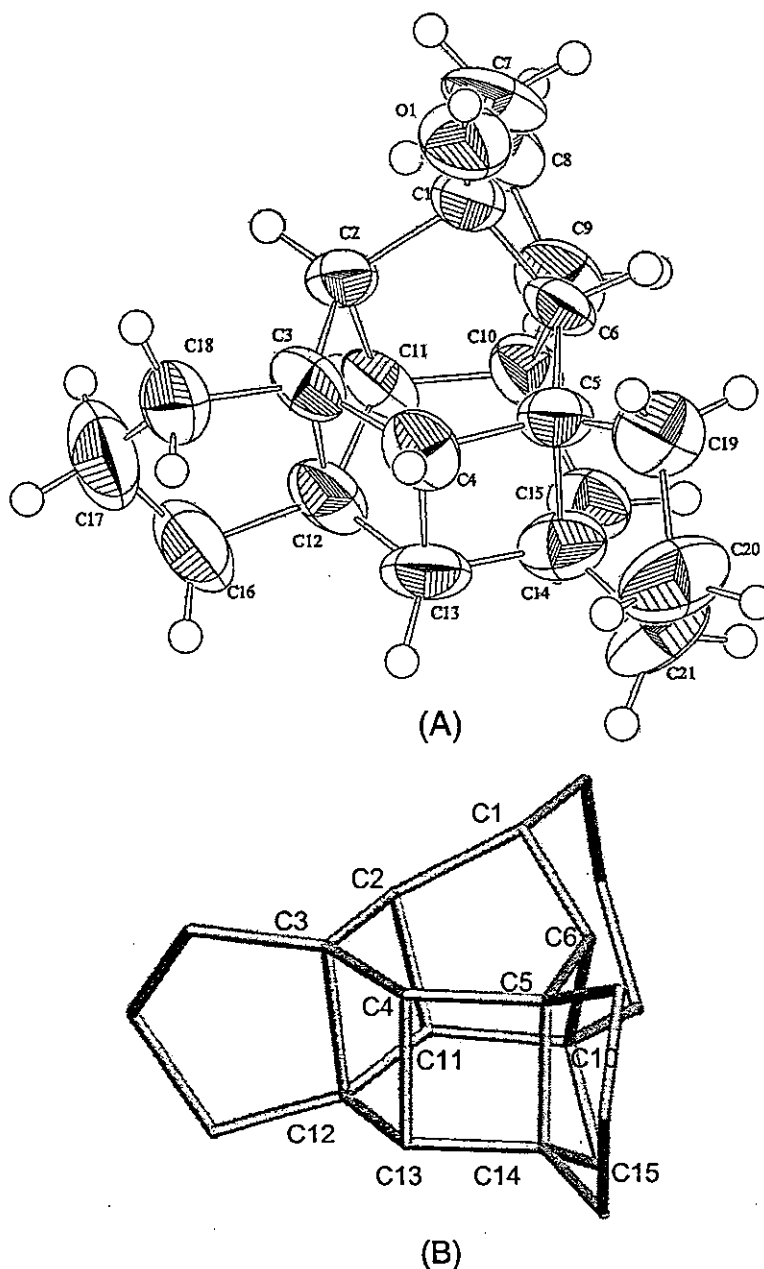
234

(A)

(B)

Figure 4. ORTEP drawings of the photoproduct 25 (−170 °C) (A) and its skeleton (B).

However, the reaction in CD₃OD in the presence of EtI (5 or 10 mol %) gave no photoproducts. In the preparative scale of the reaction, a mixture of MeOH and 2 mol/L aqueous HCl solution (17:1 v/v) (1.02 × 10⁻² mol/L) of 2 was irradiated with a sterilizing lamp in a quartz vessel for 80 min at room temperature under Ar. Separation of the reaction mixture by recycle HPLC on GPC with CHCl₃ afforded the recovered 2 (11%), the methoxy compound 26 (2.7%), as well as the dimethoxy and methoxy-hydroxy compounds 27 (11%) and 28 (5.9%) with a new caged skeleton. Prolonged irradiation gave the dimethoxy compound 27 as a major product (57%). Compound 26 has the same skeleton as 23 and 25.

In degassed nonpolar solvents such as hexane, pentane, and cyclohexane, it was found that photoreaction did not appreciably proceed. On the other hand, in the presence of dissolved oxygen in the nonpolar solvents, trace amounts of the photoproducts

oxidized at the benzylic positions 29 and 30 (yield < 0.1%) were detected. The alcohol 29 was isolated from the reaction mixture and identified by the ¹H- and ¹³C NMR (DEPT) spectra and mass spectrum. A question was raised regarding the source of this oxygen atom, oxygen gas in the solvent or singlet oxygen generated during the photoreaction. To answer this question, the reaction was conducted under the generation of singlet oxygen with 1,3-diphenyl-isobenzofuran known as a singlet oxygen monitor reagent. From this singlet oxygen reaction, the oxidized products (29, 30) were obtained in a negligibly minute quantity. Therefore, it is concluded that the oxygen atom substituted at the benzylic position came from air, not from singlet oxygen.

Next, we tested the photosensitization of the [3₃]CP 2 (2.7 × 10⁻² mol/L) containing acetone as a sensitizer (2 mg). The solution containing acetone in a Pyrex NMR tube was irradiated
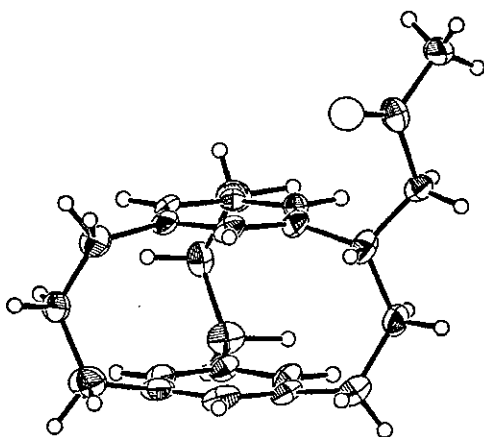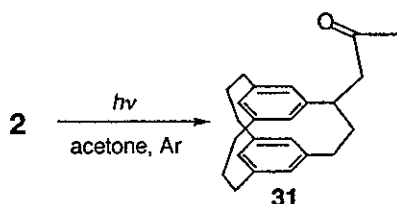
Figure 5. ORTEP drawing of 1-acetylmethyl [3₃](1,3,5)cyclophane 31 (−170 °C).

Scheme 6. Photochemical Reaction of 2 in Acetone

with a high-pressure Hg lamp (400 W) at room temperature under Ar, and the reaction was monitored by the ^{1}H NMR spectra. Irradiation of the benzene-d_6 solution of 2 for 26 h at room-temperature left 2 intact, whereas the irradiation of the CD₃CN solution for 26 h at room temperature caused some of the usual polymerization. However, in the photochemical reaction of the acetone-d_6 solution, products which could be monitored by the ^{1}H NMR spectrum were observed. In the preparative scale reaction, an acetone solution (3.6 × 10⁻³ mol/

L) of 2 was irradiated with a high-pressure Hg lamp for 6 h at room temperature. Separation of the reaction mixture by silica gel column chromatography with CH₂Cl₂ afforded 31 in a small quantity (Scheme 6). It is assumed that the irradiation of 2 formed a benzyl radical intermediate caused by abstraction of a hydrogen from a benzylic methylene group, which gave 31 by the reaction with acetone. The structure of 31 was identified as 1-acetylmethyl[3₃]CP 31 by the mass spectrum, ^{1}H- and ^{13}C NMR spectra, and X-ray structural analysis (Figure 5). The role of acetone in this photochemical reaction is not clear at the present stage. The two benzene rings of 31 are completely stacked face to face similar to that of the [3₃]CP 2, but their transannular distances are slightly longer than those of 2. The bridged carbon—carbon distance is 3.079—3.115 Å, whereas the unbridged carbon—carbon distance is 3.124—3.175 Å.

2.2. Possible Photochemical Reaction Mechanism of [3₃]-(1,3,5)Cyclophane. There has been no conclusive evidence, but we speculated a reaction mechanism (protonation mechanism) as shown in Scheme 7. The [3₃]CP 2 on irradiation in CH₂Cl₂ first gives highly strained hexaprismane derivative 18. However, protonation occurs at the unbridged carbon atom of a cyclobutane ring to give secondary carbocation 35, which rearranges to the more stable tertiary carbocation 36. Finally, 36 is intercepted by chloride or hydroxide ions to give the products 23 (X = Cl) or 25 (X = OH), respectively. One of the driving forces of a series of reactions may be the release of the steric energies. The formation of 24 can be explained by similar processes. Protonation at the unbridged cyclobutane carbon atom of the olefin 32 gives secondary carbocation 33, which rearranges to the more stable tertiary carbocation 34, and trapping the cation with water affords the olefin-alcohol 24. The protons may be generated by the photolysis of CH₂Cl₂. In fact, the pH of the reaction mixture was ca. 2 after irradiation in the wet CH₂Cl₂ solution.

Scheme 7. Expected Mechanism for the Formation of the Photoproducts 24—28ᵃ
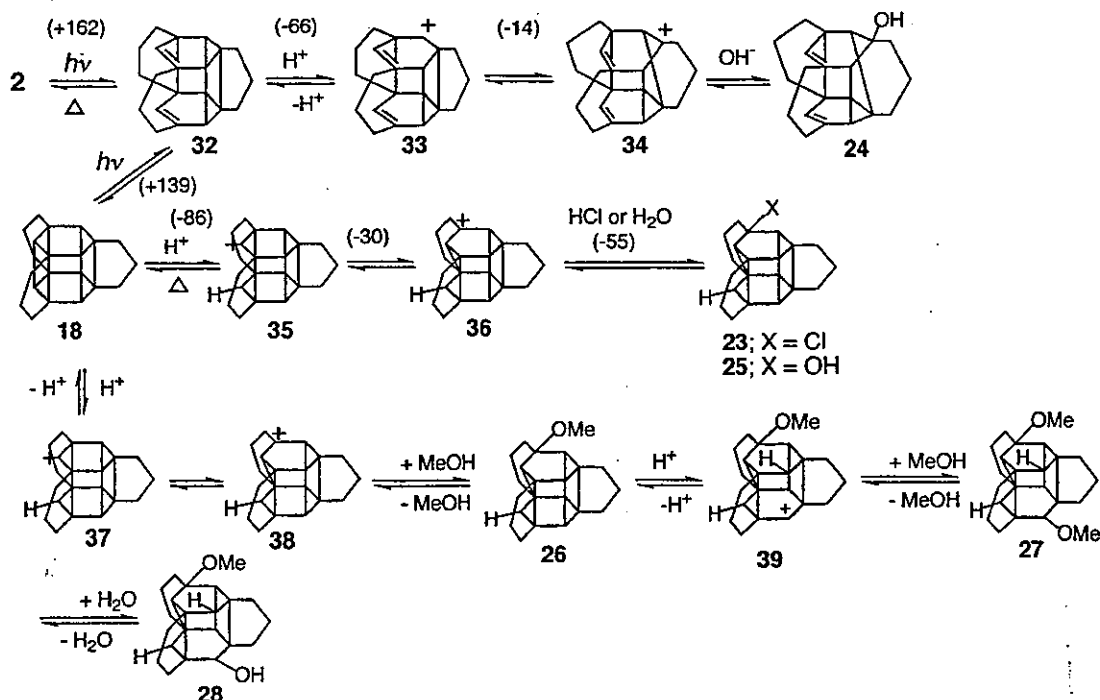
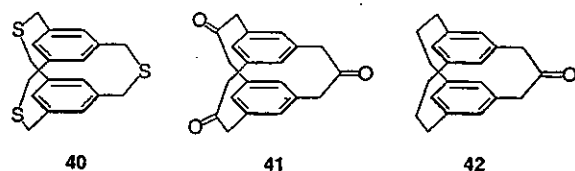ᵃ The values (kcal/mol) denote the gain or release of steric energies estimated by MM3.

Figure 6. [3₃](1,3,5)cyclophanes 40—42.

There was a possibility that 25 might be formed from 24 via [2+2] photocyclization. To examine the suggested process, a CD₂Cl₂ solution of 24 (2.38 × 10⁻⁵ mol/L) containing water (1 μL) in a quartz NMR tube was irradiated with a sterilizing lamp for 1.5 h at room temperature under Ar. The reaction was monitored by the ¹H NMR spectra. With a decrease in the signal intensity of 24, the signals due to the cyclophane 2 began to appear after 30 min, and the signal intensities increased. This result suggests that the photochemical conversion between 2 and 24 is reversible. However, after 45 min, both signal intensities due to 2 and 24 were decreased, and finally the ¹H NMR spectrum for photoproduct(s) with no aromatic or olefinic protons appeared. Thus, the olefin 24 may convert to 25 via the cyclophane 2. The direct conversion of 24 to 25 is unlikely, but the process via the cyclophane 2 is plausible.

The photochemical reaction of 2 did proceed in MeOH in the presence of a proton source to give 26 as was the case in CH₂Cl₂. Subsequent protonation to the unbridged carbon atom of the central bicyclo[2.2.0]hexane skeleton of 26 from the upper side may give the secondary carbocation 39, which is intercepted by MeOH or H₂O to give the products 27 and 28, respectively. This interception of the secondary carbocation occurred in the preferable lower side because the steric hindrance of the methoxy group and the repulsion of the lone pair on the oxygen atoms between the flag-pole bond arise if the interception occurs on the upper side. In this reaction, we were unable to isolate and characterize the highly strained propella[3₃]prismane 18, a possible intermediate, because 18 may be protonated under acidic conditions. Therefore, we studied the neutral reaction conditions using a photosensitizer. An alternative single electron transfer (SET) mechanism is also considered, and the details are described in Scheme S1 in the Supporting Information. However, this mechanism is unlikely based on the experimental results.

We investigated the photochemical reaction also in the solid state with the hope of obtaining propella[3₃]prismane 18 because protonation of the caged photoproducts would be eliminated in the solid state. A CH₂Cl₂ solution of 2 (30 mg) in a quartz test tube was evaporated to dryness in vacuo with a rotary evaporator. The resulting thin film around the wall of the test tube was irradiated with a sterilizing lamp for 6 h at room temperature under Ar. However, no apparent change was observed in the crystal color and forms, and the ¹H NMR spectrum showed complete recovery of 2. Photolysis of 2,11,20-trithia[3₃]CP 40, triketone 41, and monoketone 42 were also studied, but no reaction was observed (Figure 6).

2.3. Photophysical Properties of [3ₙ]Cyclophanes (n = 2—6). To investigate the photophysical properties of the [3ₙ]-CPs (n = 2—6), absorption and emission spectra were measured. Figure 7 shows the absorption, fluorescence and phosphorescence spectra of the [3ₙ]CPs (n = 2—6).[42] Absorption spectra were measured in degassed cyclohexane at 295 K. The absorption band at around 35 000—40 000 cm⁻¹ and a much lower
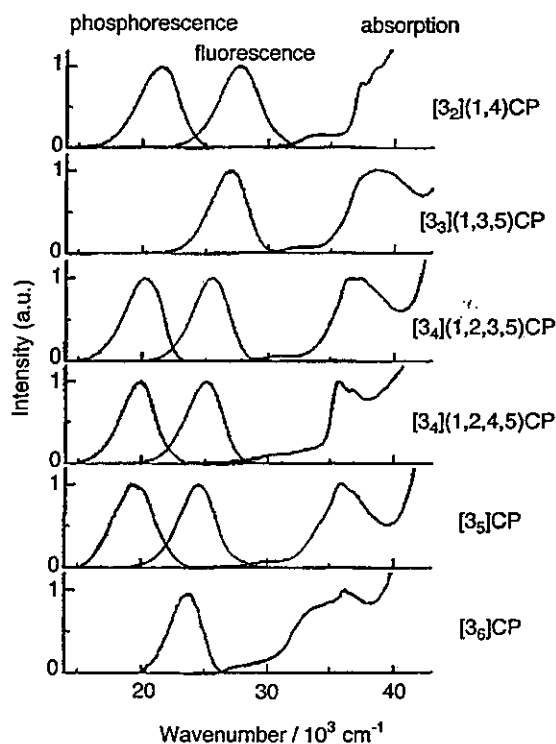

Figure 7. Absorption, fluorescence and phosphorescence spectra of [3ₙ]-cyclophanes (n = 2—6). Absorption and fluorescence spectra of the cyclophanes were obtained in degassed cyclohexane at 295 K. Phosphorescence spectra were obtained in degassed methylcyclohexane/isopentane (3:1 v/v) at 77 K.

intensity band in the region of 30 000 cm⁻¹ are observed in all cyclophanes. The former band corresponding to the "cyclophane band" gradually shifts to a smaller wavenumber region with an increase in the number of trimethylene bridges. In the photochemical reaction, the excited state was generated by irradiating this band with a sterilizing lamp. The weak absorption band is due to the transannular $\pi-\pi^*$ interaction between the two benzene rings as a benzene dimer in the ground state.[43] The appearance of this band is a characteristic phenomenon in the [3ₙ]CPs, whereas the [2ₙ]CPs (n = 2—6) and their derivatives do not show this band.

The fluorescence spectra of the [3ₙ]CPs (n = 2—6) were measured in cyclohexane at 295 K with a Hitachi F-4010 fluorescence spectrophotometer. All cyclophanes show broad fluorescence bands without vibrational structures in the region of 20 000—30 000 cm⁻¹ due to the excimer interaction.[43] It was confirmed that the fluorescence excitation spectra of the [3ₙ]-CPs agreed well with the corresponding absorption spectra. The excimeric fluorescence band shifts to a smaller wavenumber with the increasing number of the trimethylene bridges. The maximum wavelengths for the absorption and emission spectra of the [3ₙ]CPs are listed in Table 1.

The quantum yield (Φf) of the fluorescence was determined by comparing the correct fluorescence spectrum of the [3ₙ]CP with that of mesitylene in cyclohexane, which is reported to

(42) One of the reviewers suggested that Figure 7 should report the absorption coefficients of all compounds. But the low solubility of the higher members of [3ₙ]CPs, especially [3₆]CP, in cyclohexane inhibited the determination of the absorption coefficients. Absorption spectra of [3ₙ]CPs in CHCl₃ were already reported in ref 2b.

(43) Birks, J. B. *Photophysics of Aromatic Compounds*; John Wiley & Sons: New York, 1970.

237

Table 1. Maximum Wavelengths of Absorption and Emission Spectra of the [3ₙ]cyclophanes ($n = 2-6$)

compound	λ_{max}/nm[a]	λ_{max}^{fluo}/nm[a]	λ_{max}^{phos}/nm[b]
[3₂]CP 1	267	360	470
[3₃]CP 2	258	370	
[3₄](1,2,3,5)CP 3	270	390	495
[3₄](1,2,4,5)CP 4	280	400	500
[3₅]CP 5	280	405	515
[3₆]CP 6	275	420	

[a] In cyclohexane at 295 K. [b] In a mixture of methylcyclohexane/isopentane (3:1 v/v) at 77 K.

have a Φ_f value of 0.088.[44] The rates (k_f) of the fluorescence were obtained by eq 1.

$$k_f = \Phi_f \tau_f^{-1} \tag{1}$$

The lifetimes (τ_f) of the [3ₙ]CPs were determined by time-correlated single photon counting with an Edingburg FL-900 fluorescence photometer. It is interesting that the lifetime (τ_f) becomes gradually longer with an increase in the number of trimethylene bridges. The quantum yields of the [3ₙ]CPs are considerably smaller than that of mesitylene as a reference compound. The deactivation process from the singlet state to other states via intersystem crossing or internal conversion, singlet or triplet reactions may occur much more rapidly than in mesitylene. For example, the total quantum yield of the [3₃]-CP 2 during the photochemical reaction was estimated to be ca. 10^{-4}.

Phosphorescence spectra were measured in methylcyclohexane-isopentane (3:1 v/v, MP) glass at 77 K using a mechanical chopper incorporated in a Hitachi F-4010 fluorescence spectrometer. The maximum wavelengths of the phosphorescence observed are listed in Table 1. With the [3ₙ]CPs for $n = 2, 4$, and 5, broad phosphorescence spectra without vibrational structures are seen in the region of 15 000–25 000 cm⁻¹, which are considered to originate from the triplet excimer state of the cyclophanes as a benzene dimer. On the other hand, quite interestingly, phosphorescence from [3₃]CP 2 and [3₆]CP 6 was not observed at all with the Hitachi F-4010 fluorescence spectrometer.

These observations suggest that the molecular distortion, transannular strain, and distances of the two benzene rings stacked face to face are significant factors, as was suggested by the study of the triplet excimer of naphthalenophane.[45,46] Aromatic triplet excimers play an important role and show an attractive character. Lim and co-workers reported the molecular triplet excimer of naphthalene derivatives in solution.[29] It is reported that the face-to-face stacking of two fairly strained benzene rings of the cyclophanes and a sandwich-pair or parallel conformation of the tethered chromophores are favored for singlet excimers. In contrast to the singlet excimer, a triplet excimer prefers an L-shaped arrangement.[29] In the case of the [3ₙ]CPs, two benzene rings are completely stacked with each other, but a slight conformational change has to take place in the excited state when $n = 2, 4$, and 5 but not for the $n = 3$ and 6. Table 3 shows the distances of two benzene rings of the [3ₙ]-

(44) Froehlich, P. M.; Morrison, H. A. *J. Phys. Chem.* **1972**, *76*, 6(24), 3566–3570.

(45) East, A. L. L.; Lim, E. C. *J. Chem. Phys.* **2000**, *113*, 8981–8994.

(46) Yamaji, M.; Tsukada, H.; Nishimura, J.; Shizuka, H.; Tobita, S. *Chem. Phys. Lett.* **2002**, *357* 137–142.

Table 2. Quantum Yields (Φ_f), Lifetimes of Fluororescence (τ_f), Rate Constants for Fluorescence (k_f) in the Degassed Cyclohexane Solution of Mesitylene and [3ₙ]cyclophanes ($n = 2-6$) Obtained at 295 K, and the Lifetime of Phosphorescence (τ_p) in a Mixture of Methylcyclohexane and Isopentane (3:1 v/v) at 77 K

compounds	Φ_f[a]	τ_f/ns	k_f/10⁶ s⁻¹	τ_p/s
mesitylene	0.088[c]	37.3	23.6	6.3
[3₂](1, 4)CP: 1	0.012	30.3	4.0	6.0
[3₃](1, 3, 5)CP: 2	0.013	31.5	4.1	[d]
[3₄](1, 2, 3, 5)CP: 3	0.019	62.3	3.0	1.7
[3₄](1, 2, 4, 5)CP: 4	0.020	67.8	3.0	3.4
[3₅]CP: 5	0.014	116	1.2	1.2
[3₆]CP: 6	0.004	160	0.25	[d]

[a] Errors ± 0.001. [b] Determined by the equation, $k_f = \Phi_f \tau_f^{-1}$. [c] Data from *J. Phys. Chem.* **1972**, *76*, 3566. [d] No detection.

Table 3. Transannular Distances of Benzene Rings of [3ₙ]cyclophanes ($n = 2-6$).

	a (Å)	b (Å)	Δ (a – b)
[2₂](1,4)CP[c])	3.09	2.78	0.31
[3₂](1,4) CP 1	3.30	3.14	0.16
[3₃](1,3,5) CP 2	3.14	3.09	0.05
[3₄](1,2,3,5) CP 3	3.20	2.98–3.12	0.22–0.08
[3₄](1,2,4,5) CP 4	3.24	3.03	0.17
[3₅](1,2,3,4,5) CP 5	3.24	2.93–3.07	0.31–0.17
[3₆](1,2,3,4,5,6) CP 6	–	2.93	–

[a] Distances of unbridged carbon atoms. [b] Distances of bridged carbon atoms: Δ (a – b) indicates the difference between a and b. [c] Data from *J. Am. Chem. Soc.* **1954**, *76*, 6132.

CPs ($n = 2-6$) obtained by X-ray structural analyses.[6a] The transannular distances between two benzene rings of unbridged carbons (a) and bridged carbons (b), as well as the difference between them (Δ), are summarized. The benzene ring is more distorted in the [3ₙ]CPs ($n = 2$,[47] 4, 5) than in the [3ₙ]CPs ($n = 3$, 6) in the ground state. This is the reason the [3₃]- and [3₆]-CPs do not show triplet excimer phosphorescence. The order of the lifetime (τ_p) is similar to that of mesitylene, suggesting that the electronic structure of the excited triplet state is similar to that of mesitylene.

3. Conclusions

Irradiation of 2 with a sterilizing lamp in solutions of dry and wet CH_2Cl_2 gave prismane derivatives, the bishomopentaprismyl chloride 23, its hydroxy analogue 25, and the triply bridged hexacyclic dienol 24. We speculated a protonation mechanism. Irradiation of 2 would give highly strained hexaprismane derivative 18, which undergoes protonation of a cyclobutane ring to give a carbocation species. Interception of the carbocation gives photoproducts. This reaction proceeds in acidic conditions; photolysis of 2 in MeOH/2 mol/L aqueous HCl (17:1 v/v) with a sterilizing lamp afforded the new polycyclic caged dimethoxy and methoxy-hydroxy compounds 27 and 28 with a novel pentacyclo[6.4.0.0.³,⁷0.⁴,¹¹0⁵,¹⁰]dodecane skeleton 45, in addition to methyl ether 26 with bishomopentaprismane 44. Because isolation and characterization of the highly strained 18 are expected to be impossible under acidic conditions, we examined neutral reaction conditions. The reaction of 2 in

(47) (a) Gantzel, P. K.; Trueblood, K. N. *Acta Cryst.* **1965**, *18*, 958–968.
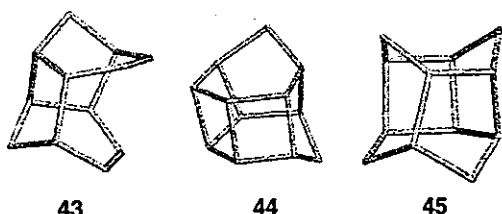
43   **44**   **45**

Figure 8. Skeletons of the new cage compounds.

acetone did not afford cage compounds except for the 1-acetylmethyl[3₃]CP **31**.

Although we have not yet succeeded in the isolation of propella[3₃]prismane **18**, we expected that **18** would be generated via the excited singlet state after irradiation of [3₂]CP **2**. Further investigations of the photochemical reaction conditions via the excited singlet state of **2**, as well as modifications of the structure of **2** in order to stabilize the hexaprismane skeleton, may lead to the isolation of the hexaprismane derivatives. The photochemical reaction of [3₆]CP **6** and fluorinated [3₃](1,3,5)-CPs are in progress, and the results will be reported soon. The photochemical reactions in the present work provide useful one-step synthetic methods leading to new polycyclic cage compounds with novel skeletons **43**—**45** from the [3₃]CP **2** (Figure 8).

All of the [3ₙ]CPs (n = 2−6) show excimeric fluorescence without monomer fluorescence. The lifetime gradually becomes longer with an increase in the number of the bridges. The phosphorescence from the [3ₙ]CPs is also observed when n = 2, 4, and 5, although it is absent for n = 3 and 6. To clarify this phenomenon in more detail, a transient absorption spectral study of the [3ₙ]CPs (n = 2−6) is in progress, and the results will be reported elsewhere.

4. Experimental Section

General Procedures. Melting points were measured on a Yanako MP−S3 micro melting point apparatus. ¹H and ¹³C NMR spectra were measured on JEOL JNM-GX 270 and AL-300 spectrometers. Chemical shifts were reported as δ values (ppm) relative to internal tetramethylsilane (TMS) in CDCl₃ unless otherwise noted. Mass spectra (EIMS ionization voltage 70 eV) and fast atom bombardment mass spectra (FAB-MAS *m*-nitrobenzyl alcohol) were obtained with a JEOL JMS−SX/SX 102A mass spectrometer. Gas chromatograph mass spectrometer was measured on a SHIMADZU GCMS-QP5050A. Electronic spectra were recorded on a Hitachi U-3500 spectrometer. Infared data were obtained on a Hitachi Nicolet I-5040 FT-IR spectrometer. Elemental analyses were performed by the Service Centre of the Elemental Analysis of Organic Compound affiliated with the Faculty of Science, Kyushu University. Analytical thin-layer chromatography (TLC) was performed on Silica gel 60 F₂₅₄ Merk and Merk Aluminumoxide 60 GF₂₅₄ neutral (TypeE). Column chromatography was performed on Merk Silica gel 60 (40−63 μm).

All solvents and reagents were of reagent quality, purchased commercially, and used without further purification, except as noted below. Aldrich anhydrous CH₂Cl₂ (99.8%) was used for photochemical reaction. MeOH was distilled from magnesium methoxide and acetone was distilled from CaSO₄.

As a light source of the photochemical reactions, we used TOSHIBA-GL sterilizing lamps (10 W × 7) in place of a low-pressure Hg lamp.

Absorption and emission spectra were measured with a U-best V-550 spectrophotometer (JASCO) and a Hitachi F-4010 fluorescence spectrometer, respectively. The samples for emission measurements were degassed on a high vacuum line by freeze−pump−thaw cycles. It was confirmed that the excitation spectra of emission from the employed

cyclophanes agreed well with the corresponding absorption spectra. The absolute fluorescence quantum yield was determined by comparing the corrected fluorescence spectra of cyclophanes with that of mesitylene in cyclohexane which is known to have a fluorescence quantum yield of 0.088.[44] The fluorescence lifetime was determined by single-photon counting method with a FL-900 CDT spectrophotometer (Edinburgh Analytical Instruments, UK).

X-ray Crystallographic Study. The X-ray structural analyses were obtain with a Rigaku RAXIS−IV imaging plate area detector with graphite monochromated Mo−K$_\alpha$ λ = 0.71070 Å) radiation and rotating anode generator. The crystal structure was solved by the direct method [SIR88][48] (**24**, **31**) [SHELXS86][49] (**25**), and [SIR92][50] (**27**, **28**), and refined by the full-matrix least-squares methods.[51] The non-hydrogen atoms were refined anisotropically, and hydrogen atoms were isotorpically. All computations were performed using the teXsan package.[52] The computations were performed with MM3(92)[53] and the Gaussian 94 program[54] graphically facilitated by Insight II from Ryoka Systems, Inc., on Silicon Graphics Octane.

Photochemical Reaction of [3₃](1,3,5)Cyclophane 2. (1) Photolysis of 2 in Dry CH₂Cl₂. A dry CH₂Cl₂ solution (650 mL) of **2** (880 mg, 3.29 mmol) in a quarz vessel was irradiated with sterilizing lamps (10 W × 7) under Ar for 150 min at room temperature. After removal of the solvent under reduced pressure, the residue was separated by SiO₂ column chromatography (hexane) to give bishomo-prismyl chloride **23** (53.1 mg, 5.2%) and the recovery of the starting **2** (352 mg, 40%). **23**: mp 68.5−70.0 °C; ¹H NMR δ 1.23 (d, *J* = 11.9 Hz, 1H), 1.47 (d, *J* = 11.9 Hz, 1H), 1.41−1.73 (m, 11H), 1.64 (s, 1H), 1.82−2.09 (m, 7H), 2.07 (s, 2H), 2.14 (d, *J* = 6.3 Hz, 1H), 2.40 (d, *J* = 6.3 Hz, 1H); ¹³C NMR (DEPT) δ 21.2 (sec.), 30.2 (sec.), 31.1 (sec.), 36.2 (sec.), 37.4 (two sec.), 38.6 (sec.), 39.7 (tert.), 40.1 (sec.), 40.7 (sec.), 42.1(sec.), 43.0 (quat.), 45.8 (quat.), 47.2 (tert.), 49.5 (tert.), 53.9 (tert.), 55.8 (quat.), 58.2 (quat.), 59.7 (quat.), 65.8 (tert.), 74.5 ppm (quat.); MS (FAB, *m/z*) 311 [M⁺-H]. Anal. Calcd for C₂₁H₂₅Cl: C, 80.62; H, 8.05%. Found: C, 80.42; H, 8.04%.

(2) Photolysis of 2 in Wet CH₂Cl₂. A water-saturated CH₂Cl₂ solution (200 mL) of **2** (800 mg, 2.89 mmol) in a quartz vessel was irradiated with sterilizing lamps (10 W × 7) under Ar for 150 min at room temperature. After removal of the solvent under reduced pressure, the residue was separated by SiO₂ column chromatography (hexane/AcOEt, 10:1) to afford polycyclic olefinic compound **24** (144 mg, 17%, *R*$_f$ = 0.30), polycyclic hydroxy dodecane **25** (47 mg, 5.4%, *R*$_f$ = 0.18), and the recovery of the starting **2** (143 mg, 18%). **24**: colorless crystals (toluene), mp 115.5−119.0 °C; ¹H NMR δ 1.34 (t, *J* = 1.6 Hz, 1H), 1.18−2.05 (m, 14H), 1.43 (d, *J* = 2.64 Hz, 2H), 2.15−2.48 (m, 4H), 2.33 (dd, *J* = 7.59 Hz, 1H), 2.53 (dd, *J* = 7.59 Hz, 1H), 2.79 (s, 1H), 5.12 (s, 1H), 5.60 (s, 1H); ¹³C NMR (DEPT) δ 20.3 (sec.), 26.3 (sec.) 28.2 (sec.), 33.8 (sec.), 33.9 (sec.), 34.4 (sec.), 35.4 (sec.), 35.7 (sec.),

(48) Burla, M. C.; Camalli, M.; Cascarano, G.; Giacovazzo, C.; Polidori, G.; Spagna, R.; Viterbo, D. *J. Appl. Cryst.* **1989**, *22*, 389−303.

(49) Sheldrick, G. M. In *Crystallographic Computing 3*; Sheldrick, G. M., Kruger, C., Goddard, R., Eds.; Oxford University Press: New York, 1985; 175−189.

(50) Altomare, A.; Burla, M. C.; Camalli, M.; Cascarano, M.; Giacovazzo, C.; Guagliardi, A.; Polidori, G. *J. Appl. Cryst.* **1994**, *27*, 435.

(51) Sheldrick, G. M. Program for the Solution of Crystal Structures; University of Goettingen, Germany, 1997.

(52) Crystal Structure Analysis Package, Molecular Structure Corporation (1985 and 1999).

(53) The computations were performed with MM3-92, graphically facilitated by CAChe from Fijitsu Ltd. MM3-Program obtained from Technical Utilization Corporation. The program was developed by N. L. Allinger and co-workers, University of Georgia. For ab initio MO calculations, the Gaussian 94 program,[54] graphically facilitated by Insight II from Ryoka Systems Inc. on Silicon Graphics Octane, was used.

(54) Frisch, M. J.; Trucks, G. W.; Schlegel, H. B.; Gill, P. M. W.; Johnson. B. G.; Robb, M. A.; Cheeseman, J. R.; Keith, T.; Petersson, G. A.; Montgomery, J. A.; Raghavachari, K.; Al-Laham, M. A.; Zakrzewski. V. G.; Ortiz, J. V.; Foresman, J. B.; Cioslowski, J.; Stefanov, B. B.; Nanayakkara, A.; Challacombe, M.; Peng, C. Y.; Ayala, P. Y.; Chen, W.; Wong, M. W.; Andres, J. L.; Replogle, E. S.; Gomperts, R.; Martin, R. L.; Fox, D. J.; Binkley, J. S.; Defrees, D. J.; Baker, J.; Stewart, J. P.; Head-Gordon, M.; Gonzalez, C.; Pople, J. A. Gaussian, Inc., Pittsburgh, PA, 1995.